The Thesis Committee for McKay Benjamin Stevens
Certifies that this is the approved version of the following thesis:

Designing Shipboard Electrical Distribution Systems for Optimal Reliability

APPROVED BY
SUPERVISING COMMITTEE:

Supervisor:

Surya Santoso

Aristotle Arapostathis

Designing Shipboard Electrical Distribution Systems for Optimal Reliability

by

McKay Benjamin Stevens, B.A.

Thesis

Presented to the Faculty of the Graduate School of

The University of Texas at Austin

in Partial Fulfillment

of the Requirements

for the Degree of

Master of Science in Engineering

The University of Texas at Austin

December 2013

Abstract

Designing Shipboard Electrical Distribution Systems for Optimal Reliability

McKay Benjamin Stevens, M.S.E.

The University of Texas at Austin, 2013

Supervisor: Surya Santoso

Analysis was performed to quantify and compare the reliability of several different notional shipboard DC distribution system topologies in serving their equipment loads. Further, the relationship between the relative placement of loads and generators within a distribution system and the system's reliability was investigated, resulting in an algorithmically-derived optimal placement configuration in the system topology found to be the most reliable in the initial analysis. Using Markov models and fault-tree analysis, system reliability indices were derived from distribution system component reliability indices, and these values were compared between competing topologies and equipment configurations.

A distribution system based on the breaker-and-a-half topology often used in terrestrial utility substations was found to be superior in terms of reliability to the currently-standard ring bus topology. Expected rates of service interruptions to equipment systems served by the breaker-and-a-half system were reduced overall, in some cases dropping dramatically to less than one expected interruption per 10,000 years.

This improvement, however, came at the expense of requiring more circuit breakers in the distribution system's construction.

Within this breaker-and-a-half distribution system, an optimal placement of loads and generators was algorithmically derived, which further improved the reliability of the system. This improvement over the base case was marginal, but the optimized placement configuration was able to reduce the expected interruption rate of the ship's radar system by over 40%.

Table of Contents

List of Tables

List of Figures

Chapter 1: Introduction

In an electric naval vessel, properly functioning equipment, such as radar, weapons, or propulsion motors, is of paramount importance to both mission success and personnel wellbeing. One key component to ensuring continuity of service for a ship's equipment is the shipboard electrical distribution system. A failure of the distribution system can result in pieces of vital equipment being left without power until repairs can be performed, potentially causing serious threats to the crew and to the mission. Therefore, it is necessary to ensure that shipboard electrical distribution systems are designed to be as robust as possible in order to minimize the frequency of service interruption.

During peacetime operations, service interruptions are most often caused by failures of individual components within the distribution system, such as prime movers, circuit breakers, or power electronic converters. In addition to peacetime equipment failure, widespread damage to distribution circuits providing electrical service to equipment during wartime is very likely. The specific scenarios in which one or more concurrent component failures will lead to a load service interruption are dependent upon the overall topology of the distribution system, as well as the relative placement of loads and generation units within the system. Previous work has been performed to establish metrics for calculating peacetime quality of service (QOS) in shipboard power distribution systems [1]. This QOS metric has been applied to shipboard power system design, but these studies have primarily focused on design choices such as generator size and control interfaces, not on comparisons of overall system topologies [2], [3].

Our work has evaluated system reliability from the perspective of the overall distribution network topology. That is, the relationship between the reliability of a

distribution circuit and the high-level topology of its connections. We seek to make explicit, quantified comparisons of reliability between competing distribution system topologies, as well as competing equipment placement configurations within these topologies. System reliability, herein, is defined by indices quantifying the expected frequency and duration of service interruptions to equipment loads caused by failures of individual components in a specific network topology. This approach to quantifying distribution system reliability as a function of system topology has been utilized in many previous works [4], [5].

Currently, most discussions of electrical power distribution in a notional electric ship utilize a distribution topology resembling the ring bus configuration often used in terrestrial power system substations. The ring bus is an attractive option for a shipboard distribution topology because it includes redundancy in distribution paths, requires a relatively small number of circuit breakers, and is readily scalable. However, reliability studies of terrestrial substations have noted that the ring bus is not the only distribution topology to possess these qualities. In particular, the Breaker-and-a-Half (BAAH) distribution topology has been found to be an overall more reliable substation design with a similar ease of scalability, though at a cost of requiring a greater number of circuit breakers than the ring bus design [6].

High-level distribution system topologies for use in an electric ship are compared in terms of reliability using a methodology combining fault-tree analysis and Markov modeling in order to derive system reliability metrics. Through these metrics, the relative reliability conferred to equipment systems by competing distribution topologies can be compared.

Several notional distribution system topologies, based upon different arrangements found in terrestrial utility substations, were designed and compared,

ultimately finding the BAAH topology to be the most reliable overall. Within the BAAH topology, further explorations were made of the relationship between system reliability and the relative placement of loads and generators within the topology. An optimized placement configuration was algorithmically derived, conferring a marginal improvement in reliability beyond the gains made through altering the overall system topology.

Chapter 2: Reliability Concepts

Reliability analysis is, in general, the evaluation of how often systems or pieces of equipment are expected to fail, and how long such a failure is expected to persist [4]. In order to quantify reliability into one or more indices, a definition of failure must be selected, along with the modes by which failure is possible. In the context of distribution systems, reliability is split into two related concepts: component reliability and system reliability.

COMPONENT RELIABILITY

Component reliability analysis assesses the expected frequency and duration of physical failures of distribution system components. While there are many components in a distribution system that can fail, this study will focus on circuit breakers, buses, and power converters. This is because we are concerned with comparing competing distribution system topologies, and the quantities and positions of these three types of components differ between topologies, while other components, such as generators, transformers, and the equipment loads themselves, do not. In this study, component failures are grouped into three types: passive failures, active failures, and stuck breakers [4] [5].

Passive failures cause the failed component to act as an open circuit, preventing power from flowing through the component. Passive failures only affect the failed component. An example of a passive failure is a circuit breaker false trip.

Active failures, also referred to as overcurrents, are caused by short-circuit faults and not only disable the failed component, but also cause all adjacent overcurrent protective devices (i.e., circuit breakers) to trip and isolate the fault. Faults propagate through buses and other pieces of equipment in the fault current's path, stopping only at

each successfully-opened circuit breaker. Examples of active failures include a bus short circuit or insulation breakdown in equipment or cables.

A stuck breaker occurs when a circuit breaker is called upon to isolate a fault but fails to operate. When this occurs, the fault propagates through the stuck breaker and must be contained by upstream breakers.

SYSTEM RELIABILITY

System reliability analysis, the focus of this work, assesses the expected frequency and duration of service interruptions to equipment loads served by the distribution system caused by component failures. Here, a service interruption to an equipment load is defined as the load being electrically isolated from all generation units.

It is important to distinguish between component reliability and system reliability. Component reliability refers to and quantifies the parameters of failures of distribution system equipment, as discussed in the previous section. System reliability refers to and quantifies the parameters of service interruptions experienced by equipment loads which are served by the distribution system. Such service interruptions are caused by component failures, but are not failures of the equipment loads themselves.

For example, consider a simple distribution system composed of a load served by a generator, separated by one circuit breaker. The circuit breaker can fail in two separate ways, actively or passively, as previously discussed (stuck breaker failure does not apply in this situation, as it must occur in conjunction with an active failure of another component). Let us say that the expected number of passive failures per year that will occur to this circuit breaker is 3, and that the average time to repair a passive failure is 1 hour. Active failures, on the other hand, are expected to occur once per year but take, on

average, 5 hours to repair. These parameters describe the component reliability of the circuit breaker.

In order to determine the system reliability of the load, we do not wish to determine how often the load itself will experience an internal failure. Rather, we seek to quantify how often the load will be electrically isolated from the generator due to failures of the circuit breaker connecting them. In our example system, the only electrical path from generator to load passes through the circuit breaker, so either a passive or active failure will cause an interruption. Therefore, we say that the expected number of service interruptions per year experienced by the load is 4 (the total number of expected circuit breaker failures of either type) and the mean time to repair of such an interruption is 2 hours (an average of the mean times to repair of the circuit breaker failures weighted by their relative frequency). These parameters describe the system reliability of the load. More detail is given on the derivation of these system reliability indices in the later section on Markov models.

The notional shipboard distribution systems examined here (see Chapter 4) serve five equipment systems: propulsion, energy storage, radar, pulsed loads (e.g., weapons systems), and zonal load centers (secondary distribution circuits serving lighting, refrigeration, etc.). The reliability of each equipment system is evaluated separately.

COMPONENT RELIABILITY INDICES

Component reliability is quantified through two indices: failure rate, denoted λ, and mean time to repair (MTTR). The failure rate is defined as the expected number of failures a given component will experience over the course of one year. The MTTR is defined as the expected length of time, in hours, that the component failure will persist

before it is repaired. The inverse of MTTR is called the repair rate, denoted π, which is given in repairs per hour.

It is important to emphasize that component failures and repairs are modeled as random processes, and the given reliability indices are the expected values of the probability distributions governing the associated failure and repair events. In general, component failure rates are not constant throughout the lifetime of a component. Instead, failure rate as a function of time is often given by the so-called bathtub curve, shown in Figure 1.

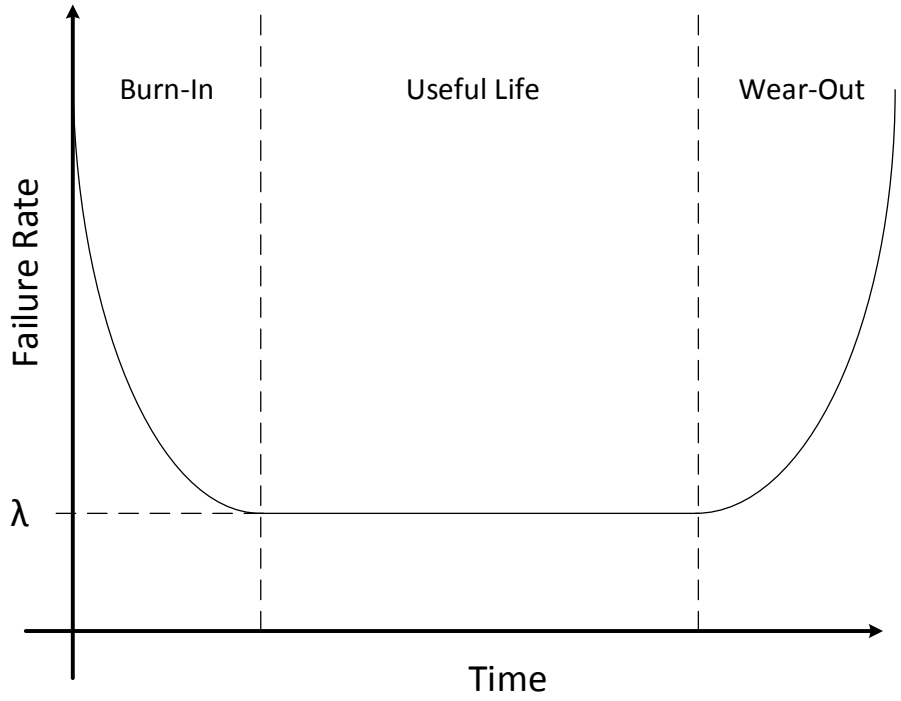

Figure 1: The bathtub curve of component failure rate as a function of time.

The higher failure rates shown at the beginning and end of the component's lifetime are referred to as the burn-in and wear-out periods, respectively. The period in the middle of the curve, in which the failure rate is constant, is referred to as the

component's useful life. We assume here that all components modeled are in their useful life period, and thus all failure rates are constant.

As a random event occurring at a constant expected rate, component failure is a Poisson process with parameter λ. Thus, the probability mass function governing the number of failures per year of a given component is given by:

$$\Pr(\mathrm{X} = \mathrm{k}) = \frac{\lambda^k e^{-\lambda}}{k!}. \quad (1)$$

The value given by (1) is the probability of the component experiencing *k* failures in one year. The expected value of this distribution is its parameter, λ. If, for example, a component is expected to experience 2.5 passive failures per year (in other words, 5 passive failures every two years), the probabilities that it will experience 0, 1, 2, 3, or 4 failures in the next year are 0.0821, 0.2052, 0.2565, 0.2138, and 0.1336, respectively. Note that the probability of a particular number of failures occurring increases as the number approaches the expected failure rate.

In addition to the number of failures experienced per year, the component failure process can also be defined by the time after a repair (or coming online for the first time) that a component will operate successfully before its next failure. This "waiting time" is given by an exponential probability distribution, also with parameter λ:

$$f(t) = \lambda e^{-\lambda t}. \quad (2)$$

As this is a continuous distribution function, we cannot refer to the probability that the component will fail at a particular time, but must instead refer to the probability that the component will fail within a given period of time. The probability that a component will fail between times t_a and t_b is equal to the integral of (2) over the interval

t_a to t_b. For example, for the component mentioned above with an expected failure rate of 2.5 passive failures per year, the probability that the component will experience a passive failure at some point in its first month of operation is given by

$$\Pr\left(0 < t < \frac{1}{12}\right) = \int_0^{\frac{1}{12}} \lambda e^{-\lambda t} dt = -e^{-\lambda t}\Big|_0^{\frac{1}{12}} = -\left(e^{-\frac{2.5}{12}} - 1\right) = 0.1881.$$

The expected value of this distribution is the inverse of the parameter, λ^{-1}. This expected value for waiting time is referred to as the mean time between failures, or MTBF. Note that component repairs are also Poisson processes, having parameter π. The expected value, then, of a component repair's waiting time exponential distribution is π^{-1}, or the MTTR.

With the exception of stuck breakers, which by definition must occur simultaneously with an adjacent active failure, component failures are assumed independent of one another.

Each type of component has one set of reliability indices for each type of applicable component failure. The values for the component failure reliability indices used in this analysis are shown in Table 1, taken either from manufacturer data or from independent testing [7], [8], [9]. Note that the failure rate of stuck breaker failures is modeled differently than other failures due to the difference described in the preceding paragraph. This is explained in further detail in the later section covering Markov models.

Component Failure	λ (failures per year)	MTTR (hours)
Circuit Breaker – Passive	0.010	4
Circuit Breaker – Active	0.010	4
Bus – Active	0.010	8
Converter – Passive	0.006	1
Converter – Active	0.006	1
Circuit Breaker – Stuck	5%	1

Table 1: Component Failure Rates.

SYSTEM RELIABILITY INDICES

Equipment system reliability is quantified through two indices: the service interruption rate, denoted μ, and the system MTTR. The service interruption rate is defined as the expected number of service interruptions that the equipment system will experience due to component failures over the course of a year. The system MTTR is defined as the expected number of hours that a service interruption will persist before service is restored through repairs to failed components. A third index, total expected downtime, is the product of the interruption rate and MTTR, defined as the expected number of hours per year that the equipment system will spend in an interrupted state.

The derivation of these system reliability indices for each equipment load is accomplished through a two-part process. First, the system's interruption scenarios are determined using fault-tree analysis. Second, system reliability indices are derived from the component reliability indices given in Table 1 using Markov models.

Fault-Tree Analysis

In order to determine how often an equipment system will be interrupted, we must first determine what circumstances will result in a service interruption to that system. An interruption scenario is a minimal set of one or more concurrent component failures that cause the load in question to become disconnected from all generators. Note that, while

there may be shared scenarios, each equipment system will have its own set of interruption scenarios. The number of individual component failures involved in an interruption scenario is called the scenario's order. Interruption scenarios up to second-order are considered, as third- and higher-order failures are exceptionally rare and therefore do not greatly affect reliability indices [4], [5].

A technique known as fault-tree analysis is used to identify a complete list of interruption scenarios for a given equipment load [10]. Fault-tree analysis is a graphical method of determining the ultimate causes of a fault event, using logical and causal links determined by the topology of the system.

A fault tree is constructed as follows. First, a fault event (in this case, a service interruption to a given equipment load) is designated by the top block of the fault tree. The most immediate (or proximate) causes of this event are identified, and each cause is given its own block, connected to the top block through logical gates. In this case, only AND and OR gates will be necessary. For each proximate cause block, further proximate causes are identified in the same manner, creating further branches of the tree. This process continues until each branch terminates in an ultimate cause. In our analysis, an ultimate cause is a component failure.

For example, consider Figure 2, a small section of the ring bus topology shown in Figure 7. If we wish to determine the interruption scenarios for the starboard propulsion system shown, we construct a fault tree. A service interruption of the propulsion system is the fault we are investigating, and so it becomes the top block of the tree (block 1). The proximate cause of this interruption, of course, is no power being supplied to the propulsion system (block 2). As this is, by definition, the only cause for the interruption in block 1, there is no need for a logical gate between the two blocks. This situation is a proximate cause, and therefore requires further branches.

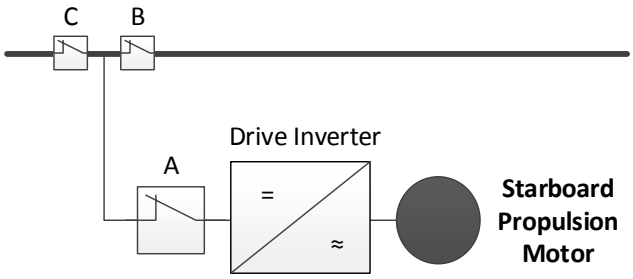

Figure 2: Section of ring bus distribution system.

It can be brought about by a number of causes. As any one of the following causes would result in a lack of power delivered to the motor, their blocks must be connected to block 2 by an OR gate. The drive inverter converting the dc power on the bus to ac power used to drive the propulsion motor could have failed. We take this to mean that there has been an internal failure of the inverter, as opposed to simply a loss of power, thus we are here referring to a component failure. This could be either a passive (block 3) or an active failure (block 4). The inverter, of course, is a power electronic device composed of a number of individual components, and thus there could be any number of internal points where these failures could originate. However, we model the inverter (along with all other components) as a lumped component and therefore assume that failures occur as described in the previous section on component failures. While an active failure on the inverter would also have secondary effects, such as causing circuit breaker A to trip, the fact that the inverter is in series with the motor means that an active failure interrupts the motor simply by virtue of disabling the inverter itself. Therefore, the secondary effects of such a failure do not need to be factored into the fault tree. These two causes are component failures, and so their respective branches terminate with their blocks.

Another possible reason for a lack of power to the starboard propulsion system is that the system's dedicated circuit breaker, labeled A in Figure 2, is in its open position (block 5). Still another possible cause is that there is no power flowing to the starboard propulsion system's outgoing line at all (block 6). That is, no power is flowing through both bus circuit breakers protecting that line, labeled B and C in Figure 2. These last two causes are proximate, and therefore require additional branches.

Note that blocks 3 through 6 appear on the same level in the hierarchy of the tree because each is a direct cause of an event confined to a single level (block 2). Obviously, the notion of a "direct cause" is somewhat arbitrary, but the causal relationships of component failures allow for a certain level of consistency in this regard. Care should be taken when constructing a fault tree to ensure that the proximate causes selected do not skip intermediate causal links in order to ensure that all interruption scenarios are identified.

This partial example, along with an additional layer of branches from block 5, is shown in Figure 3. Blocks 7 through 9 give the possible direct causes for the situation in block 5. Blocks 7 and 8 are component failures, terminating their respective branches, while block 9 is merely a proximate cause, which will require further branches. In block 9, an adjacent active failure refers to an active failure that has propagated to circuit breaker A, causing the breaker to attempt to trip and contain the failure. This could be an active failure on an adjacent component, such as circuit breakers B or C, or it could have originated on a more distant component, such as a bus, and has reached breaker A due to a stuck breaker failure. All of these possibilities will need to be accounted for in further levels of blocks.

In Figure 3, proximate causes are denoted by rectangular blocks, while component failures are denoted by diamond-shaped blocks. Each proximate cause will

continue into further branches until every branch has terminated with a component failure block.

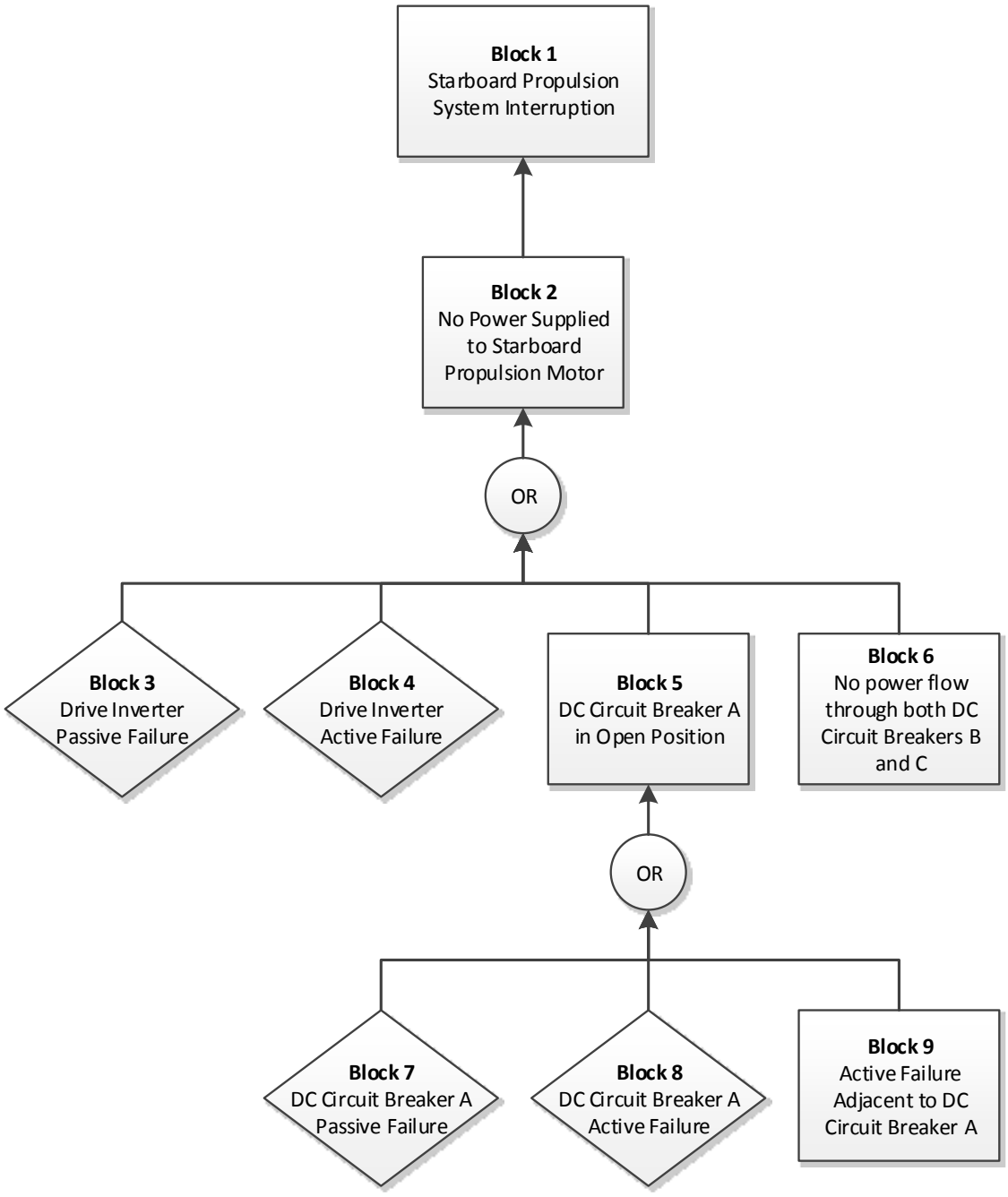

Figure 3: Partial Fault-Tree for Starboard Propulsion System.

Once the fault tree is fully constructed, each component failure that appears in the fault tree is tested to determine if it constitutes an interruption scenario. A component failure is tested by setting all instances of that failure in the fault tree to TRUE while setting all other component failures to FALSE. Then, logical paths in the fault tree are followed to determine if the top block is also TRUE, given this arrangement. If it is, the component failure being tested constitutes an interruption scenario, and vice versa. Second-order interruption scenarios are tested similarly, setting the two component failures in question to TRUE while setting all others to FALSE.

From the example in Figures 2 and 3, suppose we wish to determine whether a passive failure on circuit breaker A constitutes an interruption scenario for the starboard propulsion motor. We find the block representing this component failure (block 7), and assign it a value of TRUE, while assigning all other component failure blocks in the tree a value of FALSE. If the fully constructed fault tree for this equipment system contains multiple blocks representing this same component failure, they will all be set to TRUE. Now we follow the logical connections of the tree. Block 7 is connected to an OR gate, thus the block above it, block 5, is also TRUE. As block 5 is connected to an OR gate, the block above that gate, block 2, is also TRUE. Block 2 is directly connected to block 1, and therefore block 1 is TRUE as well. Thus, a passive failure in circuit breaker A is an interruption scenario. If following the tree's logical connections had not resulted in a value of TRUE for block 1, the component failure would not be an interruption scenario. From this method, a complete list of interruption scenarios for the equipment system can be determined.

Given that the shipboard distribution systems explored are large and complex, with a great number of components, the fault-tree analysis method described above is not performed by hand, but rather by way of a software script. Given a distribution system

topology and causal relationships for component failures, the script follows a similar testing approach to that described above, testing each set of one and two component failures in turn, thus finding a complete list of interruption scenarios for each equipment system.

Markov Models

After each interruption scenario has been identified, reliability indices are derived for the equipment system through the use of Markov models [10]. A Markov model represents a structure that can exist in one of several mutually exclusive, discrete states. Given a time constant, the model has an associated set of transition probabilities, defining the probability of transitioning from one state to another during one specified time period. In the context of distribution system reliability, different states correspond to various combinations of functioning and failed components, and transition probabilities are defined by each component's reliability indices. As this is merely a mathematical model, we are free to choose any transition time period we like. As a simplification, it is assumed that the chosen time period is short enough that at most one component failure or repair can occur per period.

For example, we can model a circuit breaker passive failure as a two-state Markov model. State one represents the functioning circuit breaker and state two represents the failed circuit breaker. The transition probability from state one to state two is the probability that the circuit breaker, which is currently functioning, will fail within one time period *T*. This probability is given by the exponential distribution shown in (2).

$$Pr(1 \rightarrow 2) = \int_{t_0}^{t_0+T} \lambda e^{-\lambda t} dt \tag{3}$$

Similarly, the transition probability from state two to state one is the probability that the circuit breaker, which is currently failed, will be repaired within on time period T:

$$Pr(2 \rightarrow 1) = \int_{t_0}^{t_0+T} \pi e^{-\pi t} dt \tag{4}$$

While this is the traditional method for using Markov models, a slightly different interpretation can be used that will allow for simpler derivations of system reliability indices and remove the arbitrary selection of transition periods from our models.

For the purposes of deriving reliability indices, it is more useful to know the probability at a given time that the model will be found in a particular state. These state probabilities, denoted p_i for state i, are functions of time. Note that these probabilities differ from those expressed in (3) and (4). The probabilities denoted in (3) and (4) represent the probability that the model will transition from one state to another within a given time period. Probability $p_i(t)$, on the other hand, represents the probability that, at time t, the model will occupy state i. In the above example, we assume that the circuit breaker is functioning at time $t = 0$, and thus $p_1(t = 0) = 1$ and $p_2(t = 0) = 0$. As time goes on, these state probabilities will change based on the probabilities of transition into and out of each state. The rate of change for state probabilities can be generalized as follows:

$$\dot{p}_i(t) = \sum_{i \neq j} \text{flowrate}(j \rightarrow i) * p_j(t) - \sum_{i \neq j} \text{flowrate}(i \rightarrow j) * p_i(t). \tag{5}$$

In this case, flowrates refer to failure or repair rates, depending on whether the transition represents a component failure or a component repair. Flows out of a state

lower the probability of being found in that state, while flows into the state raise this probability [10].

As component failure rates tend to be very small, on the order of years between failures, the long-term behavior of the model must be considered. As t approaches infinity, the state probabilities will tend to steady-state values, denoted P_i for state i. Note that (lowercase) p_i denotes a state probability that is a function of time, while (uppercase) P_i denotes the steady-state value of this probability as time approaches infinity, and is a constant value. These steady-state probabilities can be found by setting the differential term in (5) to 0.

$$0 = \sum_{i \neq j} \text{flowrate}(j \rightarrow i) * P_j(t) - \sum_{i \neq j} \text{flowrate}(i \rightarrow j) * P_i(t). \quad (6)$$

A given load's reliability indices are derived through (6) from the component reliability indices (failure rate λ and MTTR) shown in Table 1.

Each interruption scenario is simulated in a Markov model, with each state of the model representing a combination of working and failed components. Flow rates between these states are defined by the applicable component failure rates λ and repair rates π, as described above.

There are three types of Markov models used to model an equipment system's various interruption scenarios: those representing first-order scenarios, second-order scenarios that do not involve a stuck breaker failure, and second-order scenarios that do involve a stuck breaker failure.

First-Order Interruption Scenarios

In the case of a first-order interruption scenario, there are only two states: component functioning (state one) and component failed (state two). As this is a first-order interruption scenario, the occurrence of the specified component failure results in a service interruption. Thus, the equipment system to which this interruption scenario applies will be interrupted in state two of the model. In this two-state Markov model, the flowrate from state one to state two is the component failure rate λ, while the flowrate from state two to state one is the component repair rate π, as shown in Figure 4.

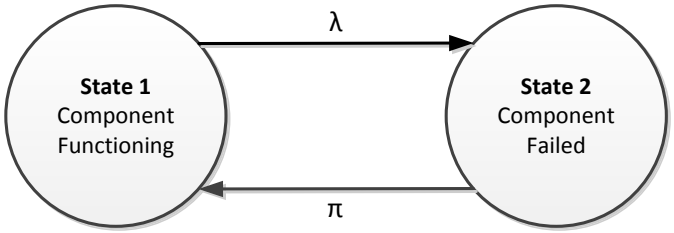

Figure 4: Markov model of a first-order interruption scenario.

For example, we earlier determined from fault-tree analysis that, in Figure 2, a passive failure of circuit breaker A is a first-order interruption scenario for the starboard propulsion motor. To model this interruption scenario, we create a two-state Markov model, with state one representing breaker A functioning properly and state two representing a passive failure of the breaker. The flowrate from state one to state two would be the circuit breaker passive failure rate found in Table 1, 0.01 failures per year. The flowrate from state two to state one would be the circuit breaker passive failure repair rate. This is the inverse of the corresponding MTTR found in Table 1, 4 hours. Thus, the repair rate is 0.25 repairs per hour. For computational purposes, the units of

time for each flowrate must match, thus the flowrate from state one to state two is converted to 0.000001142 failures per hour.

Using the values of these component reliability indices in (5), the system of differential equations governing the behavior of this model can be expressed as

$$\begin{bmatrix}\dot{p}_1(t)\\ \dot{p}_2(t)\end{bmatrix} = \begin{bmatrix}-\lambda & \pi\\ \lambda & -\pi\end{bmatrix}\begin{bmatrix}p_1(t)\\ p_2(t)\end{bmatrix}. \tag{7}$$

Therefore, the steady-state probabilities are given by

$$\begin{bmatrix}0\\ 0\end{bmatrix} = \begin{bmatrix}-\lambda & \pi\\ \lambda & -\pi\end{bmatrix}\begin{bmatrix}P_1\\ P_2\end{bmatrix}. \tag{8}$$

As states one and two are mutually exclusive, it is also known that

$$P_1 + P_2 = 1. \tag{9}$$

Substituting (9) for the bottom equation of (8), we obtain a system of two linearly independent equations and two unknowns.

$$\begin{bmatrix}0\\ 1\end{bmatrix} = \begin{bmatrix}-\lambda & \pi\\ 1 & 1\end{bmatrix}\begin{bmatrix}P_1\\ P_2\end{bmatrix} \tag{10}$$

Solving for P_1 and P_2, we obtain

$$\begin{bmatrix}P_1\\ \\ P_2\end{bmatrix} = \begin{bmatrix}\dfrac{\pi}{\lambda+\pi}\\ \\ \dfrac{\lambda}{\lambda+\pi}\end{bmatrix}. \tag{11}$$

The total scenario interruption rate μ_s is given by the component failure rate (i.e., the flowrate from state one to state two) times the probability of being in state one,

divided by the probability of not being in state two (in other words, the conditional rate of transition from the working state to the failed state, given that the system is not already in the failed state). From (9), we know that $1 - P_2 = P_1$. Thus, the total scenario interruption rate is given by

$$\mu_s = \frac{\lambda * P_1}{1 - P_2} = \frac{\lambda * P_1}{P_1} = \lambda. \quad (12)$$

The total scenario repair rate π_s is similarly given by

$$\pi_s = \frac{\pi * P_2}{1 - P_1} = \frac{\pi * P_2}{P_2} = \pi. \quad (13)$$

The total scenario MTTR is thus given by $MTTR_s = \pi_s^{-1} = \pi^{-1} = MTTR$.

In the above example of a passive failure on circuit breaker A, from (12) and (13) we find the interruption rate and MTTR of this first-order interruption scenario to be 0.01 interruptions per year and 4 hours, respectively.

The reliability indices of a first-order interruption scenario, in other words, are numerically identical to the reliability indices of the component failure that constitutes the interruption scenario. This is not surprising, given that, by definition, a first-order interruption scenario precisely coincides with its associated component failure. As a result, the interruption scenario and the component failure will occur exactly as frequently and will have exactly the same duration. Therefore, the expected frequency and average duration of both will be exactly equal.

Second-Order Interruption Scenarios Not Involving a Stuck Breaker Failure

In a second-order interruption scenario not involving a stuck breaker failure, there are four states: both components functioning (state one), component 1 failed and

component 2 functioning (state two), component 1 functioning and component 2 failed (state three), and both components failed (state four). The flowrates between these states are given by the component failure rates, λ_1 and λ_2, and repair rates, π_1 and π_2. As interruption scenarios are assumed to be minimal sets of component failures, the system will be interrupted only in state four. The Markov model for a second-order interruption scenario is visually represented in Figure 5.

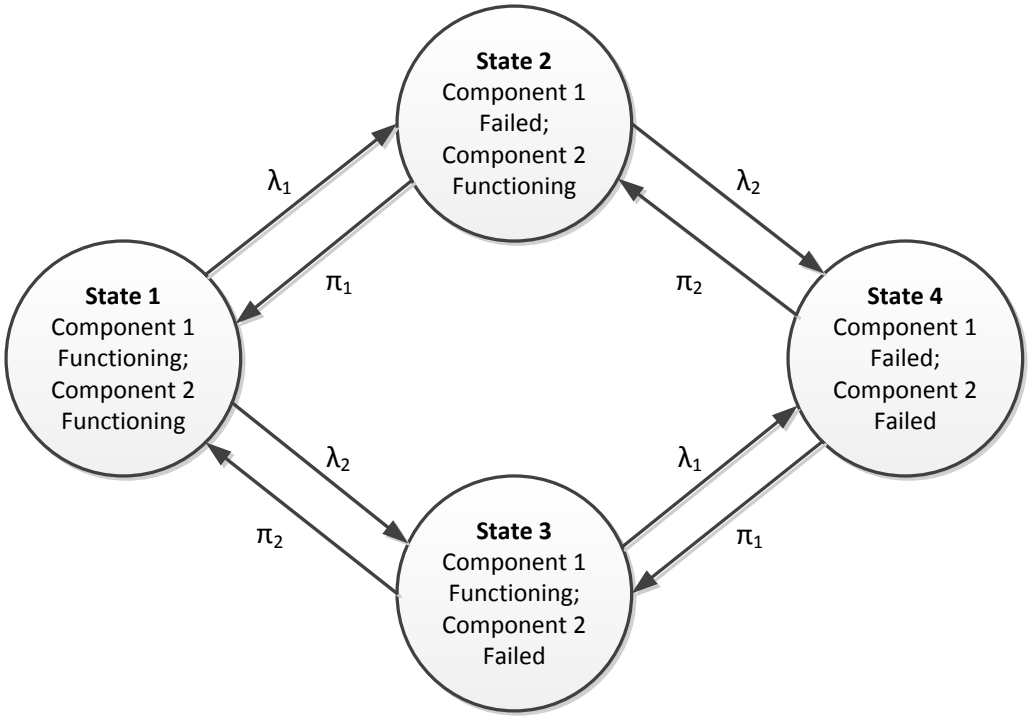

Figure 5: Markov model of a second-order interruption scenario.

For example, consider once more the portion of a distribution system shown in Figure 2. While the partial fault-tree example shown in Figure 3 did not extend far enough to cover it, we can see by inspection that concurrent passive failures of circuit breakers B and C would cause a service interruption to the starboard propulsion motor. We can also see that either one of these passive failures occurring by itself will not cause

a service interruption, as the ring bus topology ensures that power can flow in either direction through the neighboring buses. Thus, a passive failure of breaker B and a passive failure of breaker C together constitute a second-order interruption scenario.

A Markov model of this scenario would require four states. In state one, both breakers are functioning properly. In state two, breaker B has sustained a passive failure, while breaker C is functioning. In state three, breaker C has sustained a passive failure, while breaker B is functioning. In state four, both breakers are experiencing passive failures. Flowrates between states are defined by the appropriate component reliability indices taken from Table 1, as described in the previous section.

From (5), the system of differential equations governing the behavior of this model is

$$\begin{bmatrix} \dot{p}_1(t) \\ \dot{p}_2(t) \\ \dot{p}_3(t) \\ \dot{p}_4(t) \end{bmatrix} = \begin{bmatrix} -(\lambda_1+\lambda_2) & \pi_1 & \pi_2 & 0 \\ \lambda_1 & -(\lambda_2+\pi_1) & 0 & \pi_2 \\ \lambda_2 & 0 & -(\lambda_1+\pi_2) & \pi_1 \\ 0 & \lambda_2 & \lambda_1 & -(\pi_1+\pi_2) \end{bmatrix} \begin{bmatrix} p_1(t) \\ p_2(t) \\ p_3(t) \\ p_4(t) \end{bmatrix}. \quad (14)$$

From (6), the steady-state probabilities of the interruption scenario are given by

$$\begin{bmatrix} 0 \\ 0 \\ 0 \\ 0 \end{bmatrix} = \begin{bmatrix} -(\lambda_1+\lambda_2) & \pi_1 & \pi_2 & 0 \\ \lambda_1 & -(\lambda_2+\pi_1) & 0 & \pi_2 \\ \lambda_2 & 0 & -(\lambda_1+\pi_2) & \pi_1 \\ 0 & \lambda_2 & \lambda_1 & -(\pi_1+\pi_2) \end{bmatrix} \begin{bmatrix} P_1 \\ P_2 \\ P_3 \\ P_4 \end{bmatrix}. \quad (15)$$

As above, we know that the four states are mutually exclusive.

$$P_1 + P_2 + P_3 + P_4 = 1. \quad (16)$$

Substituting (16) for the bottom equation of (15), we obtain a system of four linearly independent equations and four unknowns.

$$\begin{bmatrix}0\\0\\0\\1\end{bmatrix}=\begin{bmatrix}-(\lambda_1+\lambda_2) & \pi_1 & \pi_2 & 0\\ \lambda_1 & -(\lambda_2+\pi_1) & 0 & \pi_2\\ \lambda_2 & 0 & -(\lambda_1+\pi_2) & \pi_1\\ 1 & 1 & 1 & 1\end{bmatrix}\begin{bmatrix}P_1\\P_2\\P_3\\P_4\end{bmatrix}. \quad (17)$$

Steady-state probabilities P_1, P_2, P_3, and P_4 are calculated using a software script for a given set of component failure and repair rates. Using these values, the scenario interruption and repair rates are determined by (18) and (19). For the approximation made in (18), note that P_4 is very small relative to the other state probabilities due to the fact that component failure rates are much smaller than their respective repair rates.

$$\mu_s=\frac{\lambda_1*P_3+\lambda_2*P_2}{1-P_4}\approx\lambda_1*P_3+\lambda_2*P_2 \quad (18)$$

$$\pi_s=\frac{(\pi_1+\pi_2)*P_4}{1-(P_1+P_2+P_3)}=\frac{(\pi_1+\pi_2)*P_4}{P_4}=\pi_1+\pi_2 \quad (19)$$

$$\text{MTTR}_s=\pi_s^{-1}=(\pi_1+\pi_2)^{-1}=(\text{MTTR}_1^{-1}+\text{MTTR}_2^{-1})^{-1} \quad (20)$$

For the above example of two circuit breaker passive failures, λ_1 and λ_2 are both equal to 0.01 failures per year, as given in Table 1, or 0.000001142 failures per hour. π_1 and π_2, meanwhile, are both equal to the inverse of the MTTR of 4 hours, as per Table 1, or 0.25 repairs per hour. Using (17), we calculate P_1 and P_2 to both be equal to 0.000004566. Then, from (18) and (20), we calculate the scenario interruption rate to be $9.1323\text{x}10^{-8}$ interruptions per year and the scenario MTTR to be 2 hours.

As should be made clear by comparing the reliability indices of two concurrent circuit breaker passive failures and a single breaker passive failure, second-order interruption scenarios not involving a stuck breaker failure are dramatically less frequent

than first-order scenarios, and tend to have lower MTTRs, as well. This is to be expected, given our assumption that component failures occur independently, as well as the large difference of scale between a given component failure's failure and repair rates when expressed in the same units of time.

However, second-order interruption scenarios can contribute significantly to overall system reliability indices. This is because, while there are only a few (or none, in some cases) first-order interruption scenarios for a given load, there are typically a much larger number of second-order scenarios for that load. Thus, while the interruption rate of a particular second-order scenario may be very small, the total rate of all second-order interruptions can be significant.

Second-Order Interruption Scenarios Involving a Stuck Breaker Failure

Because stuck breaker failures must occur in conjunction with an active failure, second-order interruptions involving a stuck breaker failure are modeled differently than the method described above. It is assumed that a given breaker, when exposed to an active failure, has a 5% chance of being stuck [9]. The interruption scenario, then, can be modeled as a two-state Markov model (as in a first-order interruption scenario) representing the active failure, with the resulting reliability indices adjusted to reflect this assumption. Therefore, the interruption rate of a second-order interruption scenario involving a stuck breaker and an active failure with failure rate λ is given by

$$\mu_s = 0.05 * \lambda. \tag{21}$$

Because these two failures must occur simultaneously, the service interruption will end when the first of the two failed components is repaired. Therefore, the scenario

MTTR is simply the lesser of the two component MTTRs. From the values in Table 1, this value will always equal 1 hour.

For example, in Figure 2, assume that the section of bus to the right of circuit breaker B experienced an active failure, and breaker B sticks when it attempts to trip and isolate the active failure. The failure will propagate to circuit breaker A, which will trip to contain it, interrupting service to the starboard propulsion motor. From Table 1, the failure rate for a bus active failure is 0.01 failures per hour. As there is a 5% chance that breaker B will be stuck when exposed to an active failure, the combination of an active failure on the bus and a stuck breaker failure for breaker B will occur 5% as frequently as the active failure itself, making the scenario interruption rate 0.0005 interruptions per year. These two failures occur simultaneously, and service will be restored when either one has been repaired. As repairing the bus active failure takes, on average, 8 hours, while repairing the stuck breaker only requires an average of 1 hour, the MTTR of the scenario is 1 hour.

Second-order interruption scenarios involving stuck breakers tend to occur more frequently than those not involving stuck breakers, though less frequently than first-order interruption scenarios. Their effects, however, are somewhat mitigated by their uniformly short MTTRs.

System Markov Model

Once the reliability indices for each interruption scenario of a given equipment system have been derived, the overall system reliability indices can be calculated. For a system with n associated interruption scenarios, the equipment system as a whole can be represented by a Markov model with n+1 states, as shown in Figure 6. State one represents the functioning system, while states two through n+1 each represent one of the

equipment system's interruption scenarios. The flowrate from state one to state *j* is the scenario interruption rate of the interruption scenario associated with state *j*, while the reverse flowrate is that interruption scenario's repair rate.

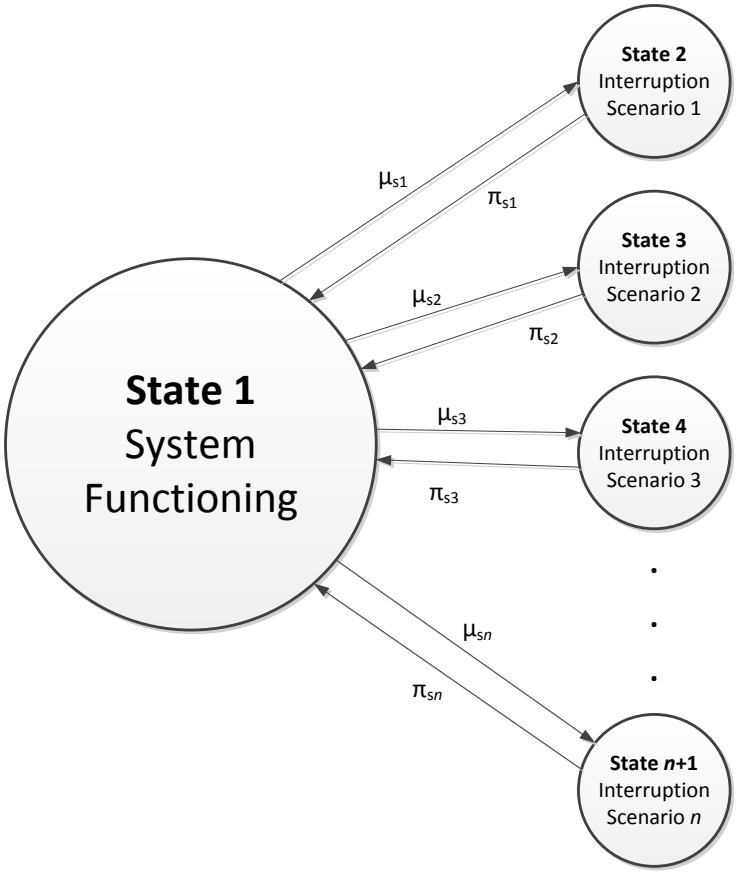

Figure 6: Markov model representing an equipment system.

Being in any state other than state one represents a system interruption, so the system interruption rate is equal to the total flowrate out of state one, the sum of the scenario interruption rates.

$$\mu_{sys} = \frac{\sum_{i=1}^{n} \mu_{si} * P_1}{P_1} = \sum_{i=1}^{n} \mu_{si} \tag{22}$$

In (22), μ_{si} is the interruption rate of the *i*th interruption scenario. Meanwhile, the total system repair rate is given by the sum of each interruption scenario's repair rate weighted by the likelihood of being in that interruption scenario's state, divided by the likelihood of not being in state one.

$$\pi_{sys} = \frac{\sum_{i=1}^{n} \pi_{si} * P_{i+1}}{\sum_{i=1}^{n} P_{i+1}} = \text{MTTR}_{sys}^{-1} \tag{23}$$

As above, π_{si} in (23) is the repair rate of the *i*th interruption scenario. Both of these values are calculated for each equipment system through a software script.

Collectively, the contents of this chapter outline a definition of system reliability that can be quantified through reliability indices, as well as describe the tools needed to derive these indices. With this definition and these tools, we may effectively and quantifiably compare competing shipboard distribution system topologies in terms of the reliability that they confer to the equipment systems they serve.

Chapter 3: Distribution System Topologies

Electrical distribution systems in electric naval vessels are composed of two levels. The high-level distribution system connects generation units to large equipment loads, as well as to zonal load centers. These zonal load centers are the lower level of the distribution system, serving a number of smaller loads. This two-tiered scheme is comparable to the relationship between distribution feeders and secondary circuits in terrestrial power delivery systems. In this study, we are concerned solely with the high-level distribution system, and accordingly zonal load centers are modeled simply as loads, disregarding their internal structure.

In each distribution system discussed here, several features remain constant. There are four generation units, two primary and two auxiliary, that serve five equipment systems: propulsion, energy storage, radar, pulsed loads (i.e., weapons systems), and zonal load centers. The four generators are all assumed to be able to power any individual equipment system on their own. Therefore, an equipment system must be isolated from all four generators in order to be interrupted. The energy storage, radar, and pulsed equipment systems each consist of a single load located at one point in the distribution system. The propulsion system consists of two loads, the starboard and port propulsion motors, each connected at separate points in the distribution system. The zonal load centers consist of four separate load centers. In these equipment systems with multiple locations, the equipment system as a whole is considered interrupted when any of the individual load locations are interrupted.

The arrangement by which the generators are connected to the loads they serve is called the distribution system's topology. There are a limitless number of possible topologies that could theoretically be used, but only a small number can or should be

used in a shipboard distribution system. In other words, some distribution system topologies are superior to others, with superiority being based on one or more selected metrics. Here, we are concerned with identifying which distribution system topologies confer the highest level of reliability to their equipment loads, as defined and quantified in the previous chapter. As a guiding set of designs, we will explore distribution system topologies based on arrangements that have been established through use in terrestrial power system substations [4] [5]. Using the tools outlined in Chapter 2, we will compare the reliability indices of these distribution system topologies in Chapter 4, determining which topology offers the highest level of system reliability.

RING BUS

The ring bus topology is the basis of most current shipboard electrical distribution systems. As the name suggests, it consists of a ring of conducting busbar, usually arranged in a rectangular shape, with several incoming or outgoing conducting lines attached. Incoming lines are attached to power sources, while outgoing lines are attached to loads. Each pair of adjacent lines is separated using a bus tie circuit breaker.

In a shipboard DC distribution system based on ring bus topology, the ring of busbar runs around the perimeter of the ship. Incoming and outgoing lines are connected to buses running along the port and starboard sides of the ship, with two cross-hull buses connected at the bow and stern to complete the ring. Some loads are connected to one point on the ring bus, while others (those spanning the width of the ship, such as zonal load centers) are connected at two different points. The notional ring bus-based DC distribution system analyzed in this study is shown in Figure 7.

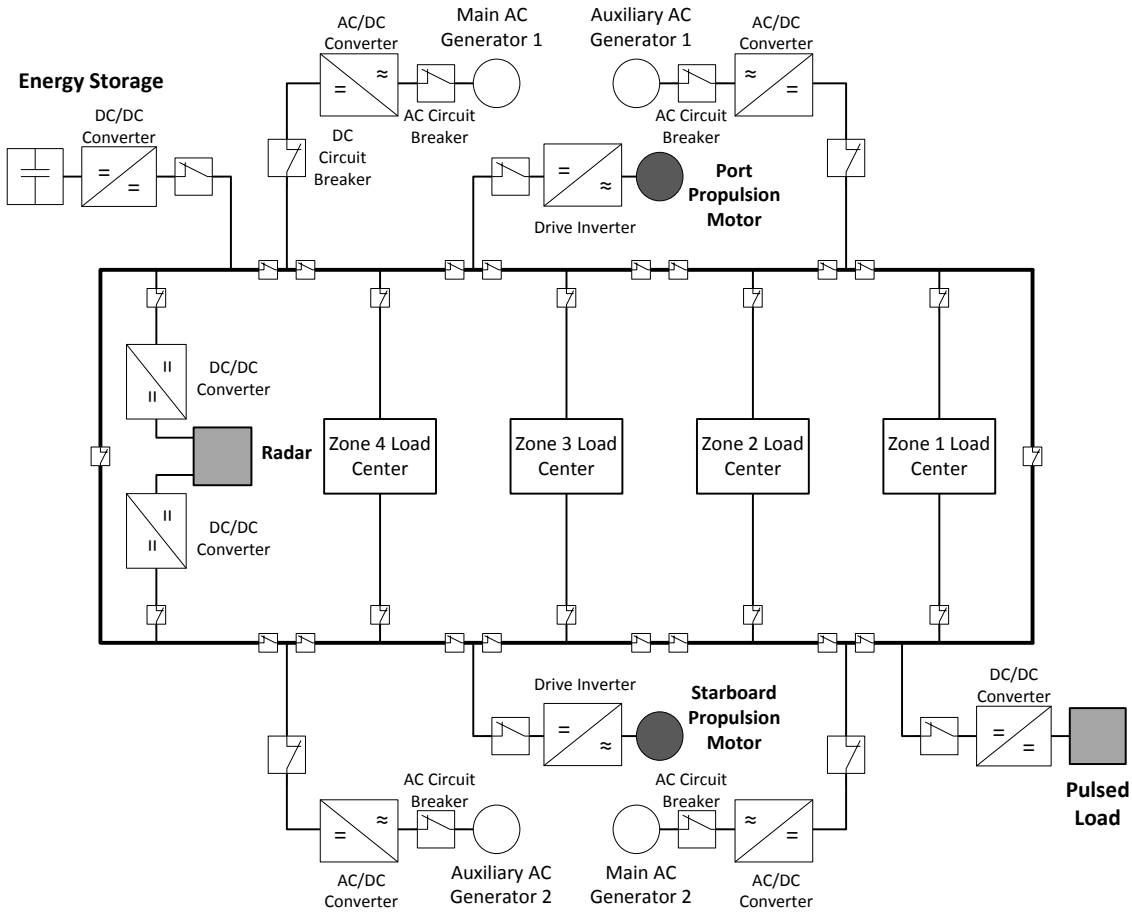

Figure 7: A shipboard distribution system with ring bus topology.

BREAKER-AND-A-HALF

The BAAH topology consists of two parallel lengths of busbar connected by several conducting lines, called bays. Each bay is attached to two lines, either incoming or outgoing, and is protected by three circuit breakers. One, called the common breaker, separates the two attached lines from each other. The other two, called the outside breakers, separate each line from its adjacent bus. As there are three circuit breakers for every two incoming or outgoing lines, each line is said to be protected by a "breaker-and-a-half". A simple representation of the BAAH topology is shown in Figure 8. Note that

each circuit breaker is outfitted with two disconnect switches. These are for maintenance purposes, and will not be drawn in subsequent figures.

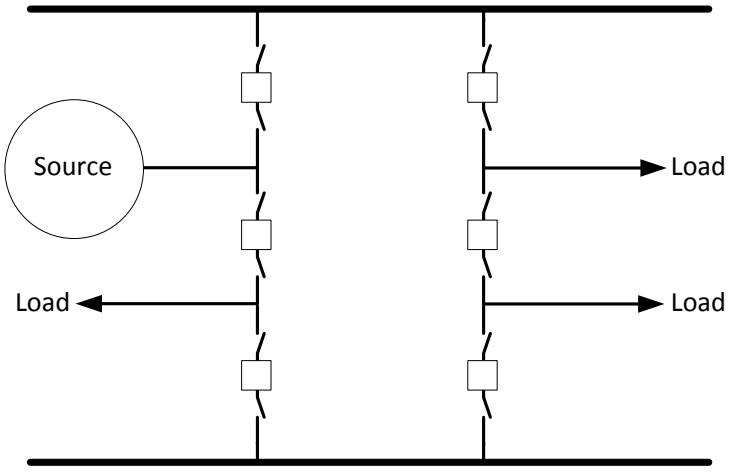

Figure 8: A simple breaker-and-a-half topology.

As shown in Figure 8, bays may be attached to two loads or to a load and a source. The placement of loads with respect to sources is especially important in a BAAH topology, as loads sharing a bay with a power source will be more reliable than those sharing a bay with another load. To illustrate this, observe the results of active faults occurring concurrently on both buses of the system in Figure 8. While the two loads on the right-hand bay will see an interruption, the load sharing a bay with the source will remain operational. In this way, vital loads can be afforded a higher level of reliability by placing them on the same bay as a generator.

In a shipboard DC distribution system based on BAAH topology, the two buses run along the port and starboard sides of the ship, with the bays running across the hull. A BAAH topology requires roughly 1.5 times as many circuit breakers as a ring bus topology with the same number of incoming and outgoing lines. As space and cost are often of great concern when designing a naval vessel, two versions of a BAAH-based DC

distribution system are analyzed in this study. Version one, shown in Figure 9, contains 34 circuit breakers, roughly the same number as the ring bus configuration in Figure 7, which contains 36 breakers. This is achieved by eliminating some of the redundant connections used in the distribution system shown in Figure 7 (specifically, those of the radar and zonal load centers). Version two, shown in Figure 10, is connected with the same amount of redundancy as the system in Figure 7, but uses a greater number of circuit breakers.

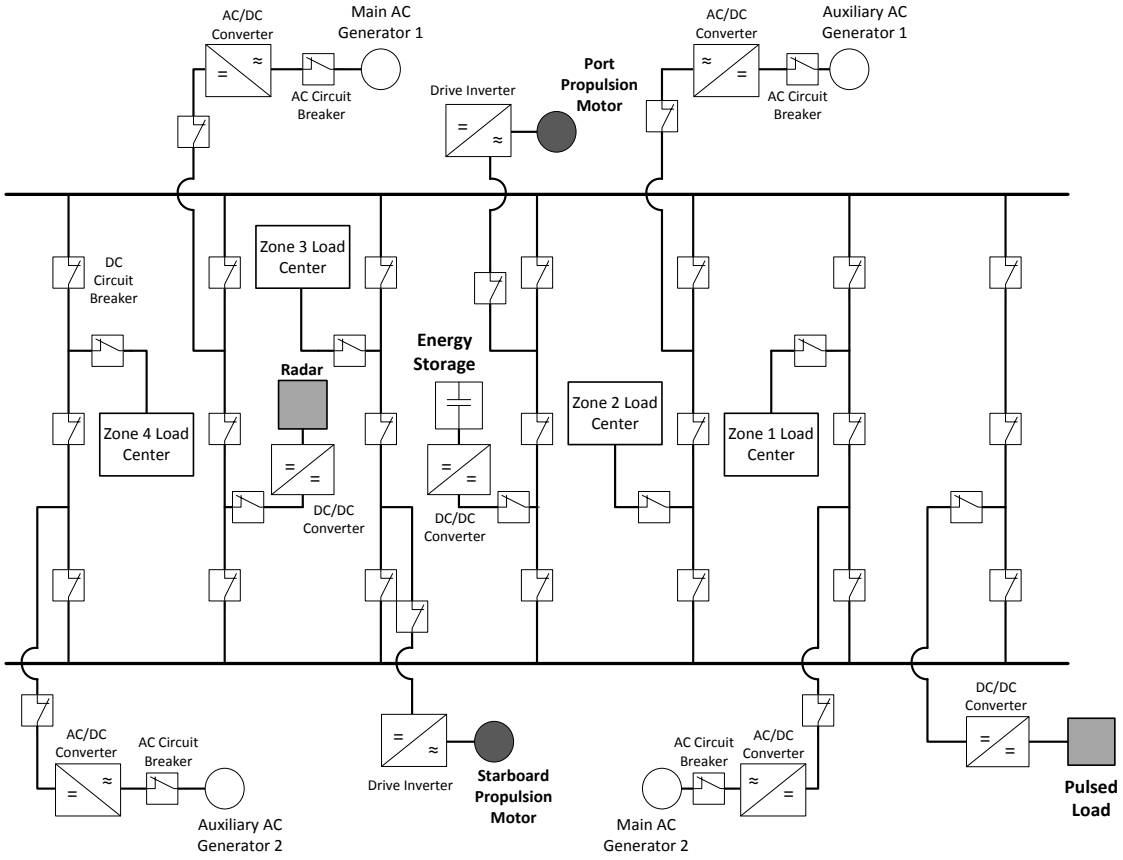

Figure 9: A shipboard distribution system with breaker-and-a-half topology (version one).

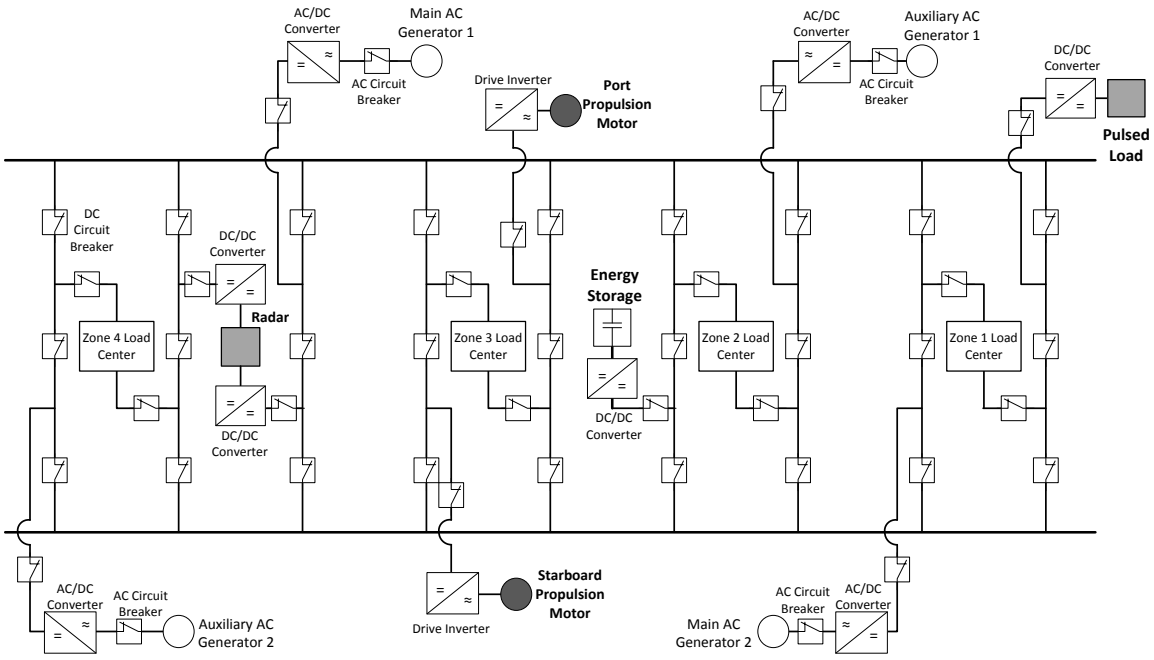

Figure 10: A shipboard distribution system with breaker-and-a-half topology (version two).

BREAKER-AND-A-HALF WITH ADDITIONAL BUS TIE CIRCUIT BREAKERS

The BAAH topology's reliability can be improved by the addition of another pair of circuit breakers used to sectionalize the buses into two halves. With this modification, active faults on a bus or an outside breaker will be confined to one side of the bus rather than propagating through the entire bus. Modified versions with added bus tie breakers of both BAAH topologies discussed above are also analyzed. In version one (Figure 9), the additional breakers are placed between bays 3 and 4, counting from the stern. In version two (Figure 10), the additional breakers are placed between bays 4 and 5, counting from the stern.

DOUBLE BUS, DOUBLE BREAKER

Like the BAAH topology, the double bus, double breaker (DBDB) arrangement consists of two parallel buses connected by cross-hull bays. In the DBDB topology,

however, each bay contains only one connecting line to a generator or load, protected by two circuit breakers, one adjacent to each bus. This topology, therefore, contains an even greater number of circuit breakers than are found in the BAAH topology. A simple comparison of the ring bus, BAAH, and DBDB topologies is shown in Figure 11.

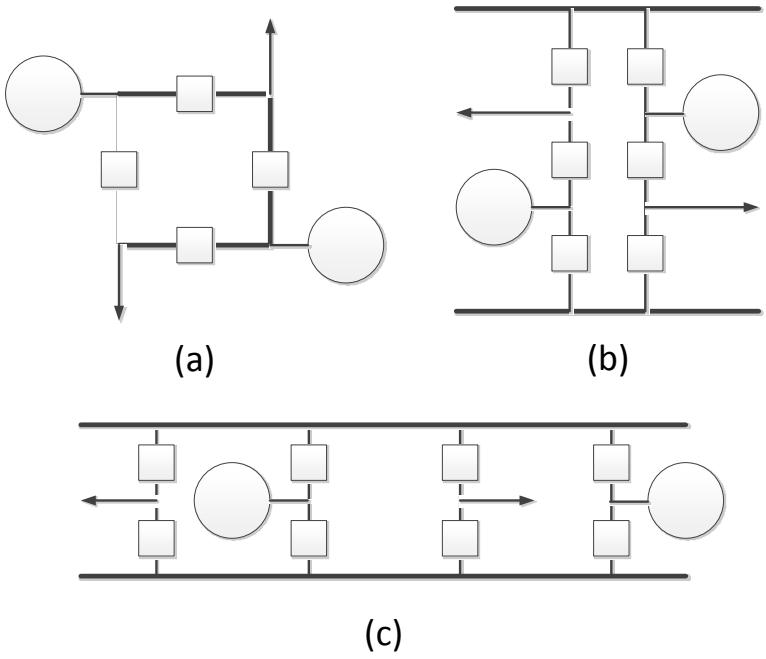

Figure 11: Comparison of (a) ring bus; (b) breaker-and-a-half; and (c) double breaker, double bus topologies.

Note that the DBDB topology was explored not with the expectation that it might be a superior topology in terms of reliability, but rather as a way to strengthen our assertion that the BAAH topology represents the most reliable configuration available. As version two of the BAAH topology (Figure 10) requires a greater number of circuit breakers than the ring bus, one may be led to believe that the increased reliability observed in the BAAH topology is merely a result of this increased number of protective devices, rather than an advantage conferred by the topology itself. The reliability indices

of the DBDB topology will serve to demonstrate that the reliability of a distribution system is not merely a function of the number of protective devices present.

For the consideration of cost and space concerns, a comparison of the number of distribution system components required for each of the topologies mentioned here is shown in Table 2.

System Topology	Number of Components Required				
	AC Breaker	DC Breaker	AC/DC Conv.	DC/DC Conv.	Drive Inverter
Ring Bus	4	36	4	4	2
BAAH v1	4	34	4	3	2
BAAH v2	4	45	4	4	2
BAAH w/ bus breaker v1	4	36	4	3	2
BAAH w/ bus breaker v2	4	47	4	4	2
DBDB	4	54	4	4	2

Table 2: System Topology Component Count Comparison.

Chapter 4: Topology Reliability Comparisons

Having selected several candidate topologies, as detailed in Chapter 3, we now seek to quantify the reliability of these topologies. Using the tools and concepts discussed in Chapter 2, we can derive a set of reliability indices for each candidate topology, quantifying the reliability each topology confers to each of its five equipment systems. Once these reliability indices have been derived, the candidate topologies can be compared and the most reliable of these topologies can be identified.

RELIABILITY COMPARISON PROCEDURE

The reliability index derivation process described in Chapter 2 is performed through a software script that represents the distribution system topology with a binary incidence matrix, each row or column representing a generator, load, or distribution system component. Fault-tree analysis is performed by simulating component failures through changes in the incidence matrix, and reliability indices are derived using the equations of the Markov model approach described in Chapter 2.

In order to facilitate simple comparisons between different topologies, a single overall interruption rate is calculated as a weighted sum of each load's interruption rate. The weights are used to reflect the relative severity of an interruption to each load. For example, an interruption to the radar or weapons system can be potentially catastrophic to crew safety or mission success, while the zonal load centers of the ship are designed such that each has a level of redundancy with respect to one another [1]. This overall interruption rate is calculated as follows:

$$\mu_{overall} = 1.5 * \left(\mu_{radar} + \mu_{pulsed}\right) + \mu_{propulsion} + 0.5 * (\mu_{storage} + \mu_{zones}) \tag{24}$$

RELIABILITY COMPARISON RESULTS

Comparisons of equipment system and overall reliability indices derived for each distribution system topology discussed in Chapter 3 are shown in Tables 3 and 4, respectively. Note that a large amount of precision in derived reliability indices is given. This will be more important for the results of the exploration of equipment placement and reliability, in which changes to reliability will be quite small. We assume that the component reliability indices given in Table 1 are arbitrarily precise, and therefore values derived from them can have a greater number of significant digits than are shown for the initial indices themselves [5], [7], [8]. Reliability index comparisons between the ring bus and various BAAH topologies are shown in Figures 12, 13, and 14.

Equipment System	Distribution System Topology	μ (interruptions per year)	MTTR (hours)	Total Downtime (hours per year)
Propulsion	Ring Bus	0.108413344	3.21388100	0.348427587
	BAAH v1	0.113011050	3.12380331	0.353024293
	BAAH v2	0.115015708	3.08683032	0.355033973
	BAAH v1 w/ bus breaker	0.110007854	3.18174544	0.350016987
	BAAH v2 w/ bus breaker	0.111010502	3.16206913	0.351022466
	DBDB	0.154034520	2.55834012	0.394072693
Energy Storage	Ring Bus	0.068501808	3.59849955	0.246503726
	BAAH v1	0.056508847	3.12375107	0.176519571
	BAAH v2	0.057512922	3.08675201	0.177528129
	BAAH v1 w/ bus breaker	0.055254589	3.17186077	0.175259863
	BAAH v2 w/ bus breaker	0.055756005	3.15235618	0.175762786
	DBDB	0.087034703	2.37920108	0.207073059
Radar	Ring Bus	0.012904640	3.32508920	0.042909080
	BAAH v1	0.056502329	3.12385345	0.176504931
	BAAH v2	0.000003868	1.86449387	0.000007213
	BAAH v1 w/ bus breaker	0.054751150	3.19175534	0.174752274
	BAAH v2 w/ bus breaker	0.000003001	1.79488659	0.000005386
	DBDB	0.020036927	1.00199000	0.020076801
Pulsed Load	Ring Bus	0.068201808	3.60992960	0.246203726
	BAAH v1	0.056008128	3.14272392	0.176018083
	BAAH v2	0.057512922	3.08675201	0.177528129
	BAAH v1 w/ bus breaker	0.054754064	3.19170405	0.174758767
	BAAH v2 w/ bus breaker	0.055756005	3.15235618	0.175762786
	DBDB	0.087034703	2.37920108	0.207073059
Zonal Load Centers	Ring Bus	0.012909001	3.32473580	0.042919017
	BAAH v1	0.175010411	3.74276599	0.655023014
	BAAH v2	0.000015982	2.12571371	0.000033972
	BAAH v1 w/ bus breaker	0.171006484	3.80695437	0.651013881
	BAAH v2 w/ bus breaker	0.000008995	2.03045685	0.000018265
	DBDB	0.026041278	1.00172538	0.026086209

Table 3: Equipment System Reliability Indices by Distribution System Topology.

Distribution System Topology	Overall Interruption Rate
Ring Bus	0.270778421
BAAH v1	0.397536484
BAAH v2	0.230055346
BAAH w/ bus breaker v1	0.387396438
BAAH w/ bus breaker v2	0.222531510
DBDB	0.371179956

Table 4: Overall Interruption Rate by Distribution System Topology.

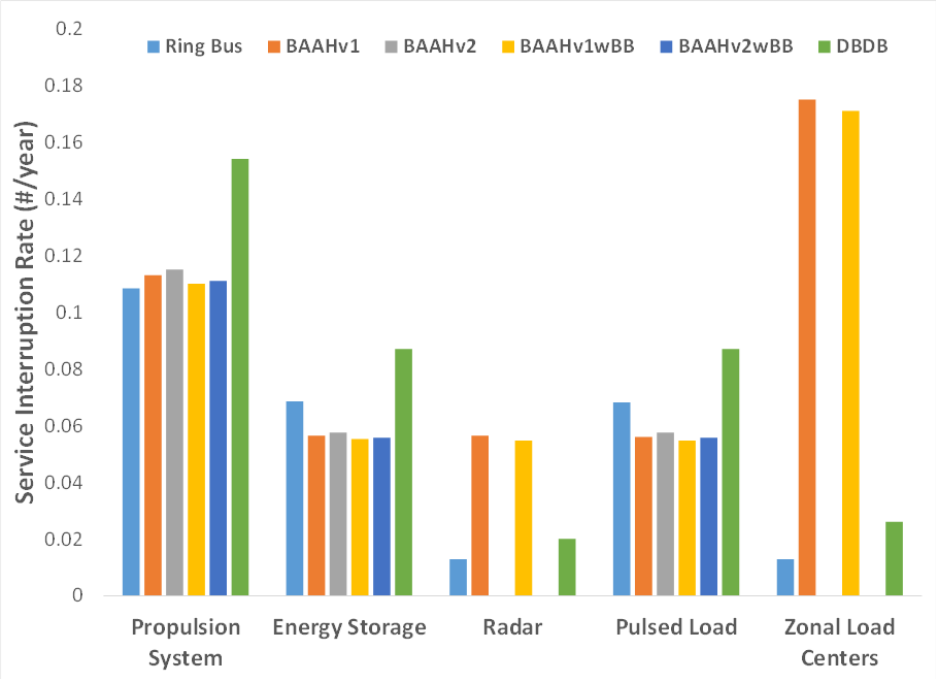

Figure 12: Equipment system interruption rate by distribution system topology.

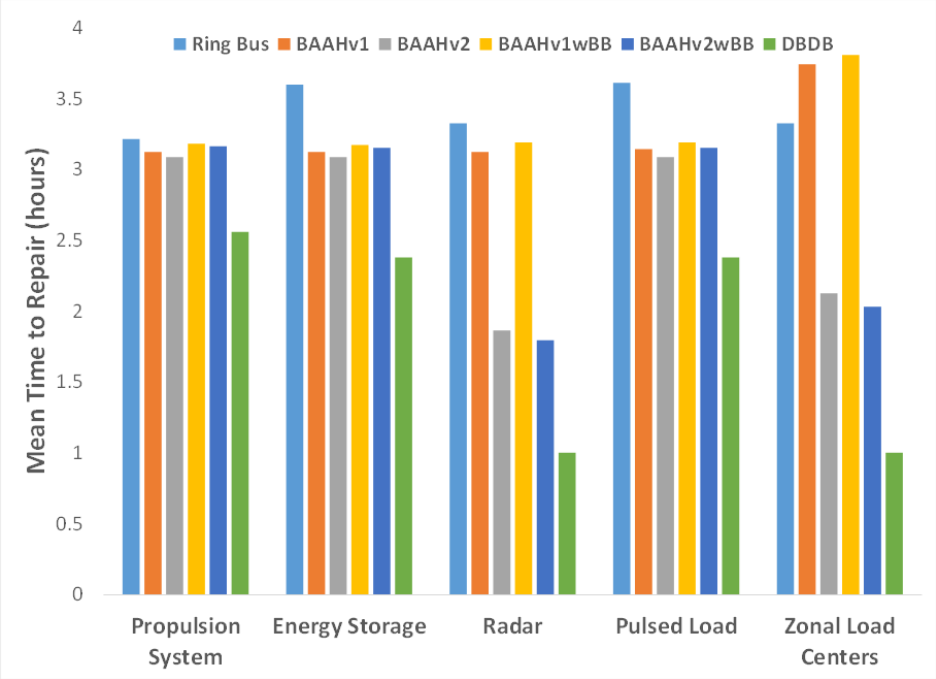

Figure 13: Equipment system mean time to repair by distribution system topology.

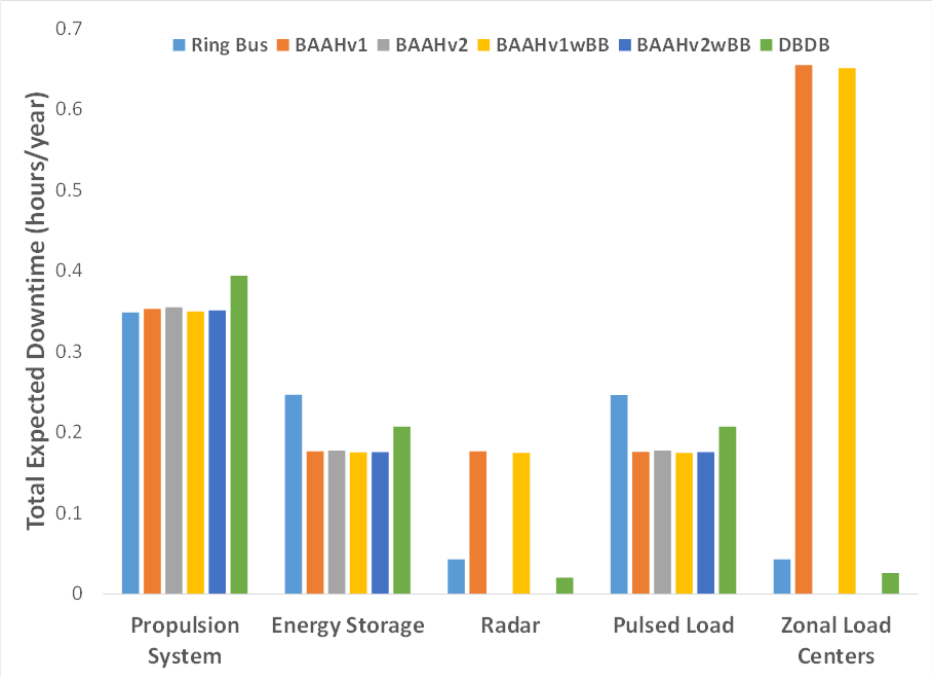

Figure 14: Equipment system total expected downtime by distribution system topology.

As can been seen, the changes in all reliability indices between topologies varies greatly with the type of equipment under consideration. For the propulsion system, the ring bus and four BAAH topologies have roughly the same level of reliability, in terms of both interruption rate (about 0.11 interruptions per year) and MTTR (about 3.1 hours). For energy storage and pulsed loads, breaker-and-a-half topologies are somewhat more reliable, lowering both the expected frequency (from about 0.068 interruptions per year for the ring bus to about 0.056 interruptions per year for the various BAAH topologies for both equipment systems) and MTTR of service interruptions (from about 3.6 hours for the ring bus to about 3.1 hours for the BAAH topologies), with almost no variation between the two different versions of the BAAH topology. This is to be expected, as these loads have no additional redundancy in conducting lines in version two as compared to version one.

For radar, version one of the BAAH topology has a significantly higher interruption rate than the ring bus topology, increasing from 0.013 to 0.057 interruptions per year, although it somewhat improves the radar MTTR. This increase in interruption rate is due to the removal of one of the redundant conducting lines to the radar system from the ring bus topology. In contrast, version two of the BAAH topology represents a marked improvement in both reliability indices over the ring bus topology, bringing the system interruption rate to a vanishingly small value, less than one expected interruption per 10,000 years. For zonal load centers, the comparison is similar, though even more exaggerated (with version one of BAAH rising to 0.175 interruptions per year), to the radar system described above, with the exception that version one of BAAH has a longer MTTR for zonal load centers than the ring bus topology.

Another interesting point to note is that the BAAH topology in general is best at supporting single-location loads, such as energy storage, pulsed loads, and radar, and

tends to offer relatively reduced protection to multiple-location loads, such as propulsion and zonal load centers. Note, for example, that the interruption rates for the propulsion system are actually very slightly worse in the various BAAH topologies than in the ring bus. This phenomenon can be seen even more clearly in comparing the interruption rates for the radar and zonal load systems in version one of the BAAH. While there is almost no difference in interruption rates between these systems for the ring bus, the zonal load centers are interrupted much more often than the radar system in the BAAH version one. This seems to be a result of the large number of circuit breakers that are incident on the buses of the BAAH. An active failure on a bus or on any of the outside breakers will cause a large number of breakers to open, thus making it more likely that an equipment system with multiple loads will be isolated due to a stuck breaker or another failure elsewhere in the system.

For each version of the BAAH topology, the addition of bus tie circuit breakers improved the service interruption rate, but the improvement was relatively minor. In some cases, the addition of a bus tie circuit breaker increased the MTTR of the system. This is because the interruption scenarios prevented by the added breakers tend to have low MTTRs (i.e., stuck breaker failures), thus bringing up the average repair time.

A comparison of service interruption rates between the ring bus, BAAH version two (which will herein simply be referred to as BAAH), and DBDB topologies is shown in Figure 15. As shown in Table 2, the DBDB topology contains a greater number of circuit breakers than both the ring bus and BAAH arrangements. If one suspected that the superior reliability over the ring bus design demonstrated by the BAAH described above was merely a matter of an increased number of protective devices, we would expect the DBDB arrangement to be more reliable still. However, as can be seen in Figure 15 and Tables 3 and 4, this is not the case. In fact, the DBDB topology has a

significantly higher interruption rate than both the Ring Bus and BAAH topologies for every equipment load. It is worth noting, however, that the DBDB topology generally provides very low MTTRs for each equipment system, owing to a large number of its associated interruption scenarios involving stuck breaker failures, which have low MTTRs. This difference in interruption rates supports the notion that the topology of the BAAH is the cause of its high level of reliability, not merely the number of components it contains. Therefore, the BAAH topology will be used in the further exploration of the effects of load and generator placement on reliability.

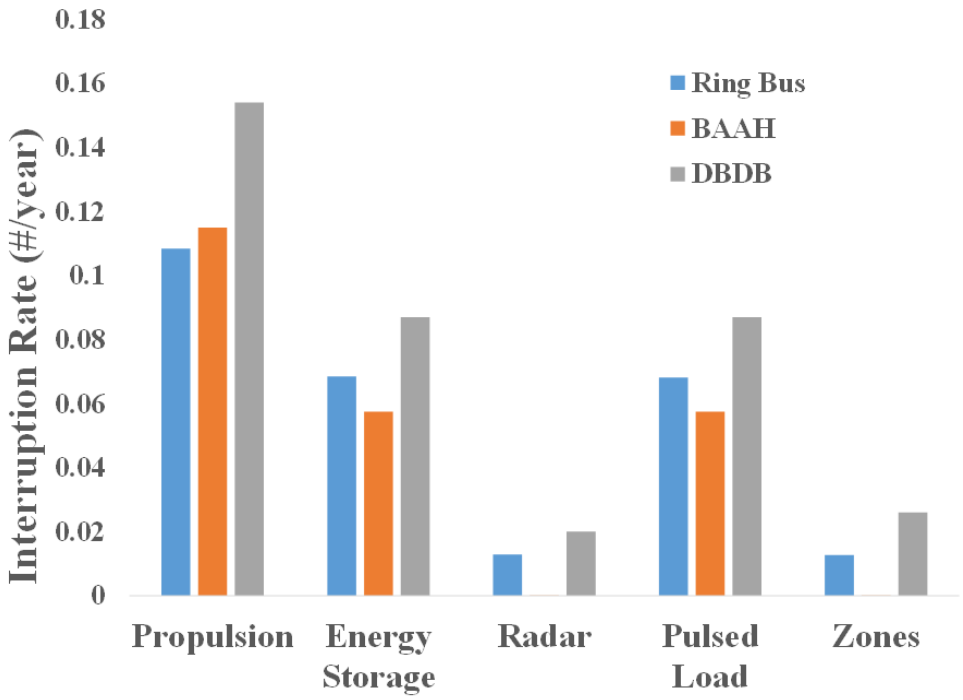

Figure 15: Reliability comparison of ring bus; breaker-and-a-half; and double breaker, double bus topologies.

Chapter 5: Equipment Placement Algorithm

It is important to note that placement of equipment loads within a distribution system is a key factor in determining service interruption rates. If, for example, the radar and pulsed loads were to be switched in position in each topology examined in Chapter 3 (holding all other connections constant), their reliability indices would also be exchanged, approximately.

Therefore, it should be noted that the reliability indices of each equipment load need not apply specifically to that load, but rather to any load that is placed in that load's position. These index exchanges will not be necessarily exact, however, due to the presence or absence of power electronic converters with different loads, and some equipment systems, such as propulsion, consisting of several loads.

This relationship between placement of loads and generators and system reliability suggests that, for any given system topology, there should be an optimal placement configuration for the system's loads and generators, for which the system's overall interruption rate will be at a minimum.

EQUIPMENT PLACEMENT ALGORITHM PROCEDURE

As mentioned in Chapter 3, in the BAAH topology (Figure 10), loads and generators are connected to cross-hull lines called bays, which are themselves connected to the buses running along the port and starboard sides of the ship. There are nine bays, each with two connection slots, for a total of eighteen slots. There are thirteen generators and loads, collectively called objects. Eight objects are connected to a single slot (the generators, energy storage unit, propulsion motors, and pulsed load), while five are connected to two slots each (the radar and the zonal load centers).

Using the configuration shown in Figure 10 as a starting point, the equipment placement algorithm makes a series of swaps, exchanging the slots of two or three objects at a time. The equipment placement algorithm is based upon the particle swarm optimization (PSO) algorithm, in which several candidate solutions, or "particles", are simulated concurrently. The PSO algorithm tracks each particle's best solution to date, as well as the global best solution to date, and each particle's iterative motion in the solution space is influenced stochastically by these best solutions. All particles eventually converge to the global optimized solution [11].

While the traditional PSO algorithm deals with continuous input functions, the algorithm can be modified to fit discrete functions in general, and optimal placement problems in particular [12], [13].

The equipment placement algorithm also simulates several candidate solutions concurrently, namely as vectors specifying which objects are connected to which slots in each candidate placement configuration. In each iteration of the algorithm, each candidate solution undergoes one swap, switching the slot positions of either two one-connection objects, two two-connection objects, or one two-connection object and two one-connection objects. Once the swap is made, the overall interruption rate of the new configuration is calculated.

The objective of the algorithm is to find the most reliable configuration of objects, thus the goal is the smallest possible value of the overall interruption rate. The algorithm, then, keeps track of the lowest overall interruption rate achieved so far by each candidate solution (the individual best configurations), as well as the lowest overall interruption rate achieved by any candidate solution so far (the global best configuration).

Before each candidate solution makes its swap, the algorithm checks to see if it is already in its individual best configuration or in the global best configuration. If it is both, the swap is random.

If it is in its individual best configuration but not in the global best configuration, the swap will either be random or be drawn from the global best solution. That is, an object is found in the global best configuration that is not in the same position in the candidate solution, and that object is swapped to the same position that it occupies in the global best solution.

If the candidate solution is in neither its individual best nor the global best configuration, the swap is either random, drawn from the global best configuration, or drawn from its individual best configuration (in the same manner as described above for the global best solution). The chances of each kind of swap occurring are summarized in Table 5.

Swap Type	**Chance of Iterative Swap if Candidate Configuration is Currently**		
	Global Best	**Individual Best**	**Neither**
Random	100%	40%	30%
From Global Best	-	60%	35%
From Individual Best	-	-	35%

Table 5: Object-Slot Swaps.

The algorithm, therefore, tends to push the candidate solutions in the direction of the best solutions found so far, while still allowing for random exploration of the solution space. In order to expedite the algorithm's progress, several configurations are prohibited, either because they obviously will not confer an improvement in reliability or

because they do not make sense from a ship-design standpoint. The prohibited configurations are any in which:

- Two generators are connected to the same bay,
- Both propulsion motors are connected to the same bay,
- Both propulsion motors are connected on either the port or the starboard side of the ship,
- Two zonal load centers are both connected to the same two bays,
- A two-connection object has both connections on the same bay, or
- A two-connection object is connected to two non-adjacent bays.

A flowchart visualizing the operation of the equipment placement algorithm is shown in Figure 16. The algorithm was executed with ten candidate solutions running for three hundred iterations each.

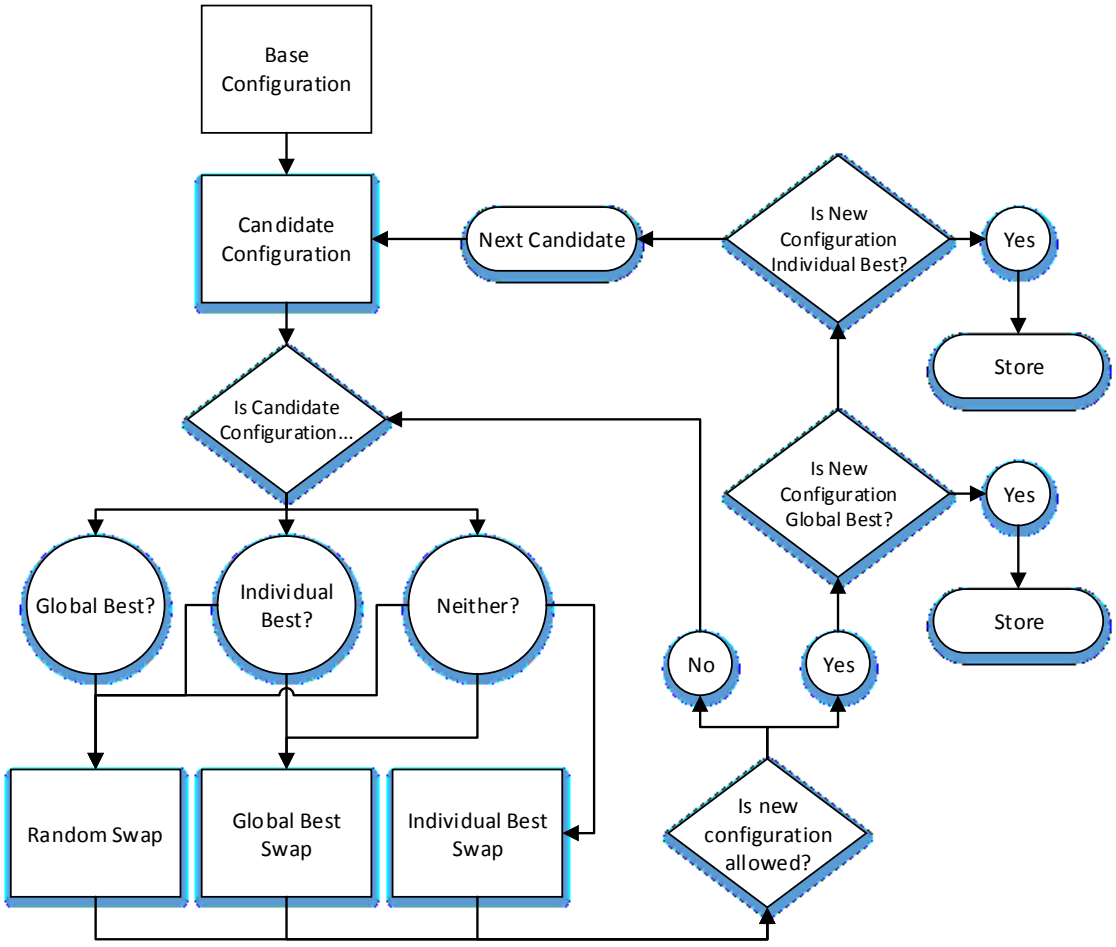

Figure 16: Operational procedure of the equipment placement algorithm.

EQUIPMENT PLACEMENT ALGORITHM RESULTS

The equipment placement algorithm identified a configuration of loads and generators within the BAAH topology that improves upon the reliability of the initial base case, shown in Figure 10. This new configuration is shown in Figure 17. The modified configuration groups the zonal load centers closer together in the middle of the ship, putting the radar at the stern and leaving the pulsed load at the bow. Generators were moved such that the pulsed load and both of the radar's connections share their bays with generation units. The improvements conferred by this modified configuration were

relatively small, suggesting that the configuration shown in Figure 10 was close to optimal to begin with. This is perhaps not surprising, as the ship design upon which Figure 10 was based was iteratively developed over time by teams of engineers with reliability as an important, if not rigorously quantified, concern [1], [2], [3].

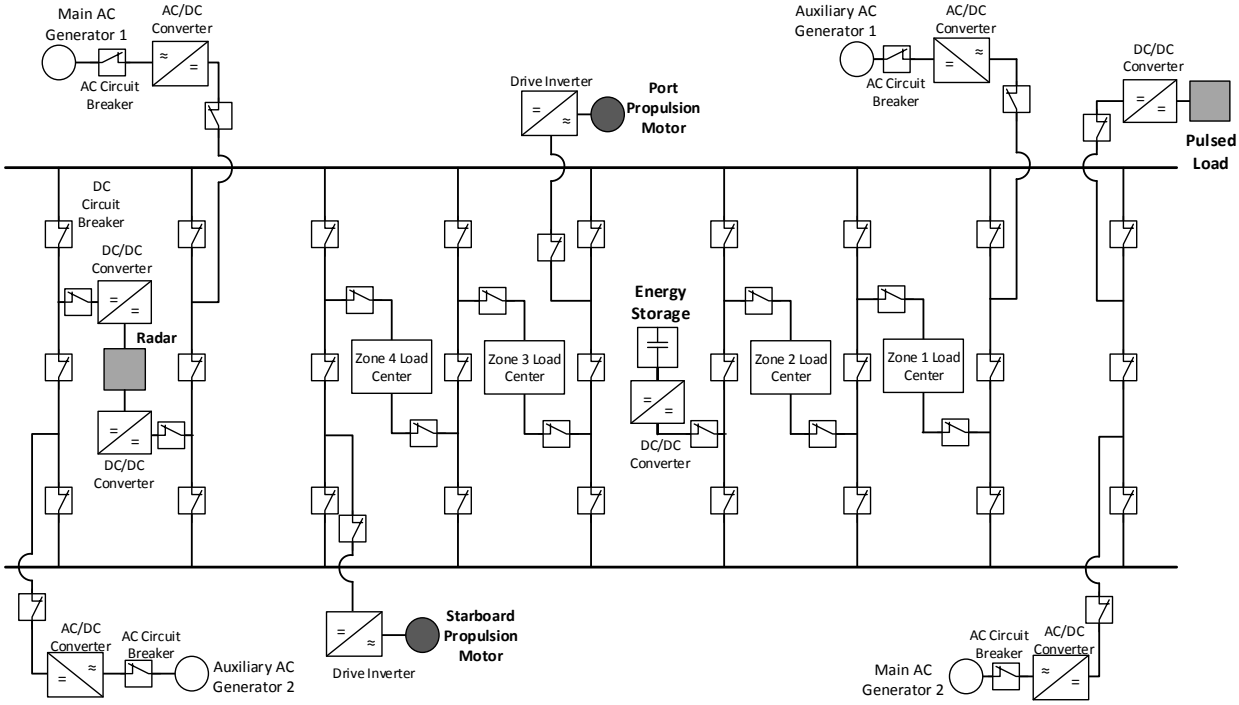

Figure 17: Optimal equipment placement within the breaker-and-a-half topology, as determined by the equipment placement algorithm.

The overall interruption rate of this modified configuration is 0.23003772, compared to the base case value of 0.23005534. Comparisons of the reliability indices of this configuration to the base case are shown in Table 6. The changes in reliability indices for the radar, pulsed loads, and zonal load centers are shown in Figures 18, 19, and 20, respectively. In these figures, a positive improvement in a reliability index refers to a decrease in the index's value, and vice versa.

	Equipment System	μ (interruptions/ year)	MTTR (hours)	Total Downtime (hours/year)
Base Case	Propulsion	0.115015708	3.08683031	0.355033972
	Energy Storage	0.057512922	3.08675200	0.177528128
	Radar	0.000003868	1.86449387	0.000007213
	Pulsed Loads	0.057512922	3.08675200	0.177528128
	Zonal Load Centers	0.000015982	2.12571371	0.000033972
Modified	Propulsion	0.115015708	3.08683031	0.355033972
	Energy Storage	0.057512922	3.08675200	0.177528128
	Radar	0.000002133	1.66866338	0.000003560
	Pulsed Loads	0.057502877	3.08690691	0.177506027
	Zonal Load Centers	0.000016073	2.12499943	0.000034155

Table 6: Equipment Configuration Reliability Index Comparison.

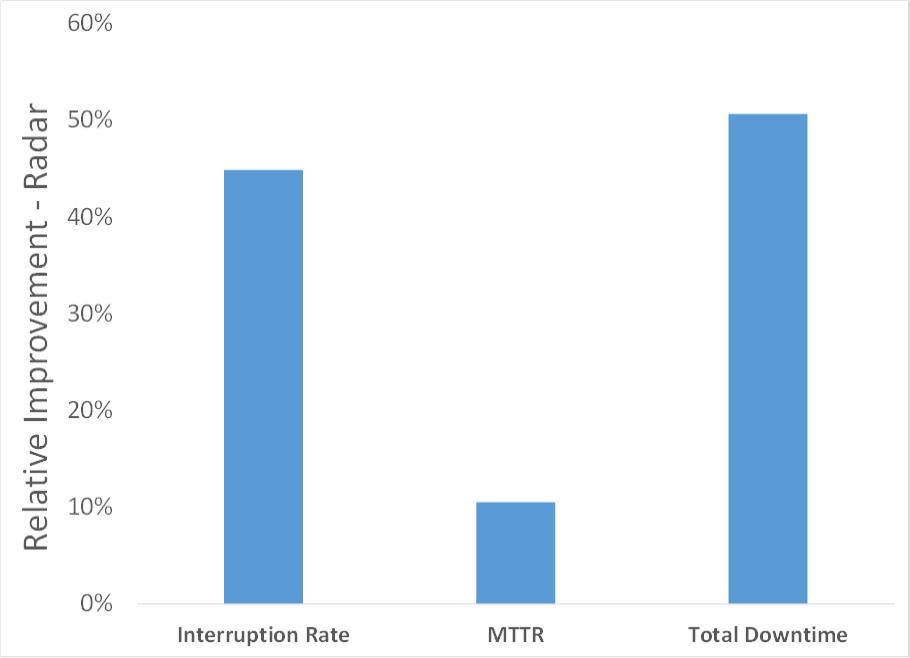

Figure 18: Changes in the radar system's reliability indices between the initial and modified equipment configurations.

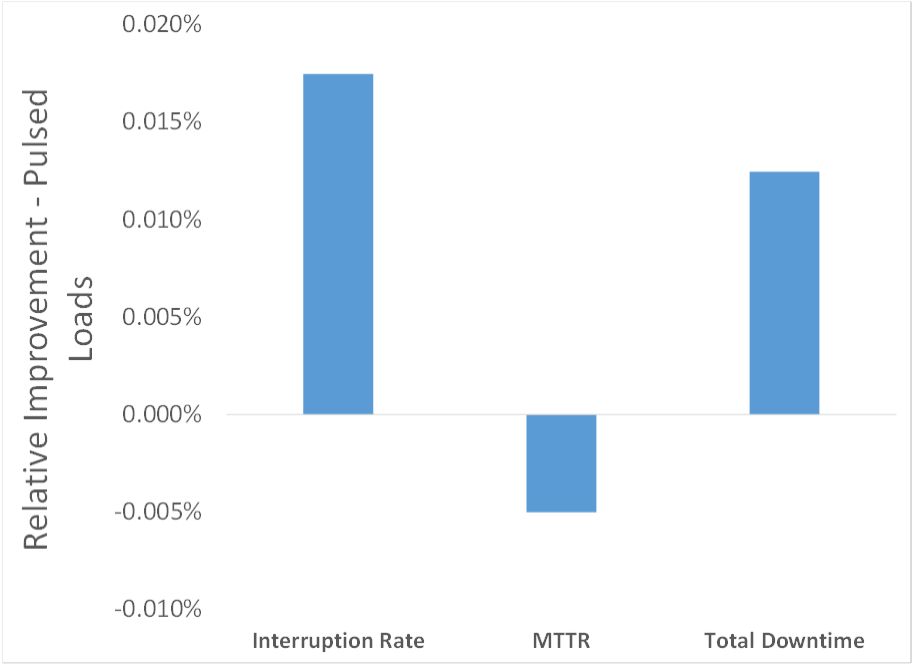

Figure 19: Changes in the pulsed load system's reliability indices between the initial and modified equipment configurations.

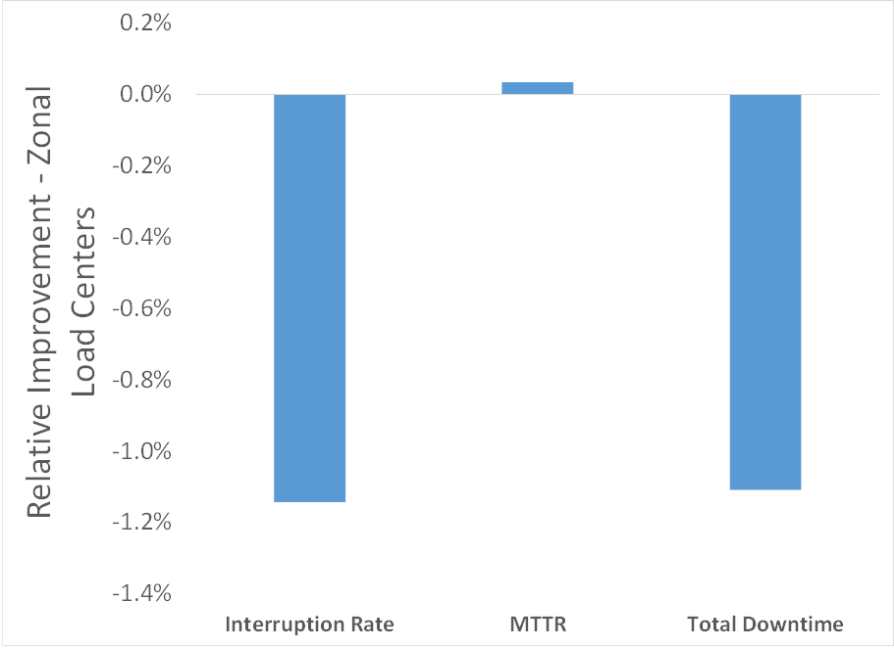

Figure 20: Changes in the zonal load center system's reliability indices between the initial and modified equipment configurations.

The reliability indices of the propulsion and energy storage systems are unchanged between the two configurations. This is to be expected, as only the starboard propulsion motor changed positions from the initial configuration, and no generators were moved such that they share a bay with any load in either system.

Radar and pulsed loads both saw reductions of their respective interruption rates. As these two interruption rates were the mostly heavily weighted in (24), the overall interruption rate that the algorithm was attempting to optimize, this is to be expected, as well. The relative improvement in interruption rate was quite significant for the radar system, while very minor for the pulsed loads. The radar system saw a significant improvement in its MTTR, as well, reducing the expected duration of service interruptions by about 12 minutes. The pulsed loads experienced a very minor increase in MTTR, but this was offset by the lower interruption rate, resulting in an overall improvement to total expected downtime.

The zonal load centers experienced a small increase in interruption rate and a very small decrease in MTTR, resulting in a small increase in total expected downtime. As the zonal load centers were lightly weighted in (24), along with the large number of slots taken up by the load centers, it is expected that the algorithm would sacrifice some of the reliability of these loads in order to improve more heavily weighted load systems such as radar and pulsed loads.

Chapter 6: Conclusions

The results demonstrate that the reliability of a shipboard electrical distribution system is fundamentally linked to the high-level topology of that system, as well as, to a lesser extent, the relative positions of loads and generators within that system. When redundancy is preserved, the breaker-and-a-half topology was shown to be the most reliable of the commonly used distribution system designs.

Compared to the ring bus topology, the breaker-and-a-half topologies analyzed here offer improvements in some aspects of equipment reliability, along with disadvantages in other areas. For version one of the breaker-and-a-half topology, improvement is seen in the reliability of the pulsed load and energy storage systems, but at a cost of reduced reliability in radar and zonal load centers. For the second version of the breaker-and-a-half topology, reliability in all systems is improved or held approximately constant, but at a cost of requiring additional circuit breakers, which may be infeasible due to cost or space concerns. Finally, the addition of bus tie circuit breakers makes slight improvements to the reliability of both versions of the breaker-and-a-half topology, but at the cost of two additional circuit breakers.

As each topology has different strengths and weaknesses in terms of reliability and cost/space, this comparison should allow designers of shipboard electrical distribution systems to tailor a ship's distribution topology to the equipment requirements of the ship's future missions, as well as its physical dimensions and budget constraints.

Further, the results of the equipment placement algorithm show that there are further gains in reliability that can be achieved through optimized placement of equipment loads within a distribution system topology. These gains are relatively small compared to those that are achieved through choice of overall topology, but changes in

equipment placement are easier and less costly design choices to implement than changes in system topology. Placement choices also do not affect the number of required distribution system components, as can be the case with choices of system topology.

To facilitate any further research performed on this topic, a flexible software tool has been developed over the course of this work. Given a set of matrices and vectors specifying the topology of a distribution system, the tool can derive a set of reliability indices for each load in the system. If desired, the tool can also apply the equipment placement algorithm to the topology using a specified number of candidate solutions and iterative steps, outputting an optimally reliable configuration of loads and generators within the topology. A more detailed discussion of this software tool is found in the Appendix.

For any distribution system, reliability can be optimized through a combination of overall topology choice and the placement of loads and generators within the topology. The demonstration of the breaker-and-a-half topology's superior reliability and the equipment placement algorithm developed here are important tools in the design of any distribution system in which reliability is a key concern.

Appendix

The system reliability analysis performed in this work can be recreated and expanded upon through a series of software scripts developed in MATLAB. Please contact Professor Surya Santoso for further information or access to these scripts.

The front-end program is titled Reliability_Analysis_Main.m and, when run, opens a series of input prompts. First, the program requests that the user select a distribution system topology from a list. The list currently includes the six system topologies analyzed in Chapters 3 and 4. When a topology is selected, the program will load data specifying the type and relative position of each component, load, and generator in the chosen topology. Arrays are also created specifying the objects and slots of the topology, as defined in Chapter 5.

These arrays are housed in a set of functions that are called by the main program, each corresponding to a different topology. The six pre-written topology functions are RingBus.m, BAAHv1.m, BAAHv2.m, BAAHv1wSB.m, BAAHv2wSB.m, and DBDB.m. Any new topologies that one wishes to investigate using this tool should be made in the same format, following the conventions specified in each of these files.

The main program also loads a set of arrays specifying the reliability indices of the component failures, as shown in Table 1. These are loaded by calling the function found in comp_rel_indices.m. Any changes to the values found in Table 1 should be performed in this function.

The main program then performs reliability analysis on the five equipment systems of the chosen distribution topology, though calling the function reliability_calc.m. For each equipment system, this function produces a service

interruption rate and MTTR, as well as an overall interruption rate index, as defined in (24).

First, the reliability calculation function identifies the various interruption scenarios for the current equipment system, through the function FaultTree.m. This function tests every possible set of one and two concurrent failures that can occur in the topology, simulating failures through alterations to the incidence matrix of the topology. After each failure or failures are simulated, a check is made to determine if the load(s) of the equipment system is isolated from the topology's generators (i.e., the failure(s) under consideration constitutes an interruption scenario).

After this list of scenarios is generated, scenario reliability indices are derived for each scenario, through the function Markovscen.m. This function uses the relevant equations found in Chapter 2 to derive scenario interruption rates and MTTRs for each interruption scenario. These scenario reliability indices are then passed to the function Markovsys.m, which calculates the system interruption rate and MTTR for the equipment system. After this process and been repeated for each equipment system, the overall interruption rate is calculated, and the system reliability indices are displayed.

The main program then asks if the user would like to apply the equipment placement algorithm to the topology in order to derive an optimized equipment configuration. If the user agrees, they specify a number of candidate topologies to be simulated and a total number of iterations to be executed, as described in Chapter 5. The algorithm runs as shown in Figure 16.

Swaps are made by altering each candidate topology's incidence matrix, with the specific components to be altered being specified by the object and slot arrays. The function object_slot_index.m creates an array that can be used for the purpose of making swaps and checking to make sure each potential swap constitutes a valid configuration.

The specifics behind each type of swap and the valid configuration check are housed in a series of functions. As each type of topology has a potentially different set of rules governing the swaps and the check, each has its own function. The relevant functions are random_swap_{topology}.m, individual_best_swap_{topology}.m, global_best_swap_{topology}.m and check_{topology}.m. At the conclusion of the algorithm, the program outputs a list specifying which slot each object is attached to in the optimized configuration, as well as the system reliability indices and overall interruption rate of the optimized configuration.

If new topology files are introduced, new swap and check functions will have to be written as well to accommodate the specifics of the new topologies.

References

[1] N.H. Doerry and D. Clayton, "Shipboard Electrical Power Quality of Service," IEEE ESTS, July 2005.

[2] N.H. Doerry, "Designing Electrical Power Systems for Survivability and Quality of Service," ASNE Naval Engineers Journal, Vol. 119, No. 2, 2007, pp. 25-34.

[3] N.H. Doerry and J.V. Amy Jr., "Implementing Quality of Service in Shipboard Power System Design," IEEE ESTS, 2011.

[4] M.S. Grover, R. Billinton, "A Computerized Approach to Substation and Switching Station Reliability Evaluation", University of Saskatchewan, November 1973.

[5] R.N. Allan, M.F. de Oliveira, "Reliability Modeling and Evaluation of Transmission and Distribution Systems", PROC. IEEE, Vol. 124, No. 6, June 1977.

[6] Z. Liu, "Reliability Analysis of Breaker Arrangements in High Voltage Stations: A Fault Tree Analysis," Chalmers University of Technology, 2008.

[7] R. E. Brown, G. Frimpong, and H. L. Willis, "Failure Rate Modeling Using Equipment Inspection Data," IEEE Trans. Power Systems, vol. 19, no. 2, May 2004.

[8] Y. Wu and W. Chang, "A Study on Optimal Reliability Indices in an Electrical Distribution System," Proc. IEEE Power System Technology, vol. 2, 2000, pp. 727-732.

[9] R. E. Brown, J. R. Ochoa, "Distribution System Reliability: Default Data and Model Validation," IEEE Trans. Power Systems, vol. 13, no. 2, May 1998.

[10] P. M. Anderson, *Power System Protection*, IEEE Press, 1999, pp. 1052-1248.

[11] J. Kennedy and R. Eberhart, "Particle Swarm Optimization," Proc. IEEE International Conference on Neural Networks, vol. 4, pp. 1942–1948, Piscataway, NJ, 1995.

[12] K. Prakash and M. Sydulu, "Particle Swarm Optimization Based Capacitor Placement on Radial Distribution Systems," Proc. IEEE PES GM, 2007.

[13] O. Amanifar, "Optimal distributed generation placement and sizing for loss and the reduction and voltage profile improvement in distribution systems using particle swarm optimization and sensitivity analysis," Proc. IEEE EPDC, 2011.